

JSCMT

Journal of Sustainable Construction
Materials and Technologies

Journal of Sustainable Construction Materials and Technologies

YEAR: 2021 | VOLUME:06 | ISSUE:01



e-ISSN: 2458-973X



Contents lists available at YTUEJS

Journal of Sustainable Construction Materials and Technologies



<https://jscmt.org/>

E-ISSN: 2458-973X

Editor In Chief

Assoc. Prof. Dr. Orhan CANPOLAT
Yildiz Technical University

Assistant Editor

Khizar NAZIR
Yildiz Technical University

Contact

Journal of Sustainable Construction
Materials and Technologies (JSCMT)
Yildiz Technical University
Civil Engineering Department, 34220 Esenler
Istanbul – Turkey
Web: <http://dergipark.gov.tr/jscmt/>
E-mail: jscmt@yildiz.edu.tr



Honorary Editorial Advisory Board

Tarun R. NAIK
University of Wisconsin-Milwaukee, USA

Editor-In Chief

Orhan Canpolat
Yildiz Technical University, Turkey

Co-Editors

Rakesh KUMAR
Central Road Research Institute, India

Benchaa BENABED
University of Laghouat, Algeria

Editorial Board

Messaoud SAIDANI
Coventry University, UK

Xiaojian GAO
Harbin Institute of Technology, China

Mustafa ŞAHMARAN
Hacettepe University, Turkey

Mohiuddin M KHAN
Washington State University, USA

Roman RABENSEIFER
Slovak University of Technology in Bratislava, Slovakia

Soofia Tahira Elias ÖZKAN
Middle East Technical University, Turkey

Ali Naji ATTIYAH
University of Kufa, Iraq



Contents lists available at YTUEJS

Journal of Sustainable Construction Materials and Technologies



E-ISSN: 2458-973X

<https://jscmt.org/>

Asad-ur-Rehman KHAN
NED University of Engineering & Technology, Pakistan

A.S.M. Abdul AWAL
Universiti Teknologi Malaysia, Malaysia

Aravind Krishna SWAMY
Indian Institute of Technology Delhi, India

Mohammed Mosleh SALMAN
College of Engineering Al-Mustansirya University, Iraq

Mohammed ARIF KEMAL
Aligarh Muslim University, India

Sepanta NAIMI
Istanbul Aydin University

Language Editors

Mohiuddin M KHAN
Washington State University, USA

Mukhallad M.M. AL-MASHHADANI
Istanbul Gelisim University, Turkey

Assistant Editor

Khizar NAZIR
Yildiz Technical University, Turkey






TABLE OF CONTENTS

Title	Pages
Research Articles	
Rubberized Mortar from Rubber Tire Waste with Controlled Particle Size <i>Diego David Pinzón Moreno, Sebastião Ribeiro, Clodoaldo Saron</i> DOI: https://doi.org/10.29187/jscmt.2021.54	1-11
Influence of Marble Powder and Fly Ash on Rheological Properties and Strength of Cementitious Grouts <i>Hikmet Sis, Tufan Kiyak, Cenk Fenerli, Mehmet Genç</i> DOI: https://doi.org/10.29187/jscmt.2021.55	12-23
Investigation of Mechanical and Permeability Properties of Fiber Mortars <i>Veysel Akyüncü</i> DOI: https://doi.org/10.29187/jscmt.2021.57	29-35
Review Articles	
Sustainable Practices in Bridge Construction <i>Balaji Venkateswaran</i> DOI: https://doi.org/10.29187/jscmt.2021.56	24-28
Pollution Free and Sustainable Copper Production Using Greenhouse Gas CO ₂ <i>Subir Paul, Ramesh Chandra Das, Tamal Das</i> DOI: https://doi.org/10.29187/jscmt.2021.58	36-43



Research Article

Rubberized Mortar from Rubber Tire Waste with Controlled Particle Size

Diego David Pinzón Moreno^{a, }, Sebastião Ribeiro^{a, }, Clodoaldo Saron^{a,*, }

^aDepartment of Materials Engineering, Engineering School of Lorena, University of São Paulo, LOM-EEL/USP, Polo Urbo Industrial, Gleba AI-6, s/n, CEP: 12602-810, Lorena, SP, Brazil

Abstract

The generation of new materials such as rubberized mortar presents itself as an alternative to the decrease environmental problems generated due to the inadequate management of scrap tires, reaching high economic potential and environmental sustainability. In this study, mortar composites were prepared from Portland blast-furnace slag cement (type IS) and rubber granular waste from unusable tires of different commercial-brands with the purpose of evaluating the effects of the rubber particle size and rubber content on mechanical, chemical and morphological properties of the composites. Rubberized mortar has shown considerable improvement in flexural strength, strain and apparent density when compared to the conventional mortar, while the size particle of the rubber caused insignificant changes on these properties. Thus, rubberized mortar shows promising potential for the use of the material in applications where flexural strength is essential.

Keywords: Mortar; Rubber; Tire; Recycling; Particle Size; Composites

1. Introduction

The inappropriate disposal of scrap tires causes serious environmental problems worldwide [1,2]. The global tire manufacturing output was estimated at over 17 million tonnes in 2016 with providing an annual growing nearly at 4% through 2022 [3]; these tires will eventually become solid waste with pollutant potential [4].

On the other hand, some alternatives have been employed to minimize the problem such as reuse of tires by retreading, burning for energy recovery, recycling and application as ground rubber products, recycling by devulcanization methods and pyrolysis for generation of several products [1-6]. Thus, the greater number of alternatives for consuming of scrap tires contributes to a decrease the amount in tires waste in the environment. In this sense, the incorporation of tire rubber particles in materials widely used in the world such as asphalt and mortar is very interesting. Moreover, news materials with modified properties can be generated for specific applications [7].

Studies on the development of mortar or concrete composites with rubber aggregates of different sizes, morphologies and treatments have been performed, causing interest in different commercial and academic sectors [8-13]. Naturally, the use of polymeric aggregates in cement matrix generates challenges on the material due to the difficulty in obtaining interface adhesion between phases of different chemical characteristics. In the production of mortars and concretes, the pozzolanic activity of the cement plays a fundamental role in the final properties. However, there is not a chemical reaction between the rubber aggregates and the cement, preventing the improvement of properties in the generation of mortars and concretes rubberized [11, 14-17]. Therefore, the content rubber, as well as the particle size of the rubber, incorporate in the mortar can result in considerable variation in the performance of the material properties. Thus, the aims of this present study have been to evaluate the effects of

This paper was recommended for publication in revised form by Editor Sepanta Naimi

**Corresponding author/E-mail address: saron@usp.br (C. Saron)*

<https://doi.org/10.29187/jscmt.2021.54>

Received 6 February 2020; Received in revised form 3 September 2021; Accepted 5 September 2020,

Available online 31 March 2021



low rubber content and of the rubber particle sizes on the properties of rubberized mortar prepared with commercial Portland cement and recycled rubber from scrap tires.

2. Experimental

2.1. Materials

For rubberized mortar preparation, it was used commercial Portland blast-furnace slag cement (type IS), according to the ASTM C595 [18], manufactured by the Companhia Siderúrgica Nacional (CSN), sand as an aggregate of natural source from the Paraíba do Sul river basin, which is classified as medium and pre-washed, and rubber waste obtained from the tire retreading process when the tire covering is partially scraped and cut by means of a process with rotary knives, generating a rubber waste in elongated granular form. The tires are from different brands, leading to an unspecified composition of the rubber waste.

2.2. Materials preparation

Before preparation of the composites, the sand was sieved to remove impurities and to define the particle size distribution, which was verified between 150 to 600 μm , ensuring the homogeneity and reproducibility of the samples. On the other hand, before mixing the mortar, the moisture content in the sand was evaluated in order to correct the water trace in the case of having considerable water contents in the aggregate, trying to maintain the proportions of the constituents of the mortar without variation at the mixing time. Additionally, the rubber waste was sieved to the separation of different particle sizes.

The mortar preparation was performed in a mechanical mixer, Metal Cairo AG-5: 2008, with spindle rotation and planetary movement. Firstly the water was added to the vat, which was followed by cement, sand and rubber, respectively. All conditions for mortar blending were based on ASTM C305 standard [19].

Specimens were prepared for axial compressive and flexural tests. Thus, seven compositions for flexural test and seven other compositions for the axial compressive test were prepared, in addition to the reference compositions for each type of test. Three granulometric ranges of rubber were used for each composition. Table 1 describes the samples identification based on the content and particle size of the rubber in the different compositions. Table 2 shows the ratio of components used in the preparation of the mortar for all the compositions, following recommendations of the standard practice ASTM C305 [19].

Table 1. Samples identification

Rubber Content (wt%)	Fine particle size rubber (0.85 to 1.68 mm)	Medium particle size rubber (1.68 to 2.38 mm)	Coarse particle size rubber (2.38 to 3.38 mm)
0	R	R	R
1	S1	M1	L1
2	S2	M2	L2
3	S3	M3	L3
4	S4	M4	L4
6	S6	M6	L6
8	S8	M8	L8
10	S10	M10	L10

Table 2. Mortar components

Component	Proportion by weight (kg)	Percentage (wt%)
Cement	1,00	23,64
Sand	2,75	65,01
Water	0,48	11,35

All compressive and flexural sample molds were sealed with adhesive and tape to ensure tightness. At the same time, all the molds were covered with a light coat of oil to ensure the proper demolding of the specimens. Immediately, the material was placed in the molds in the shortest possible time, after mixing. For each sample, the material was placed in three layers receiving each layer 30 uniform strokes with an ordinary socket. This molding is completed by placing each of the samples on an automatic vibrator Sieve agitator at 3600 vibrations/min (vpm) for 1 minute. After molding, the material was pre-cured and cured in according to standard practice ASTM C109 [20]. For the development of the mechanical tests, the specimen's surface was firstly ground and polished in horizontal grinding Ferdimat machine T42:2005-600 mm.

2.3. Characterization

Axial compressive and flexural tests, scanning electron microscopy (SEM), X-ray fluorescence (XRF), surface area analysis (BET), and apparent density (AD) were performed for characterization of mechanical, chemical and morphological properties of the material.

Axial compressive and flexural tests were performed in a universal electromechanical test machine (maximum load of 100 kN) EMIC-DL10000/700 at a speed of 0.5 mm/min, using four specimens for each mix design, according to the recommendations of the standard practice ASTM C109 [20].

For the flexural test, the three-point flexural strength (S_f) was calculated by equation 1, according to the recommendations of the standard practice ASTM C348 [21].

$$S_f = 3PL/2bh^2 \quad (1)$$

Where P is the maximum force that supports each test specimen, L and the distance between supports, b is the length of the base of the specimen and h is the height of the specimen. The average compressive strength (S_f) was obtained by the numerical average of the four specimens previously tested.

SEM micrographs were obtained in a HITACHI TM3000 equipment, employing secondary electron signal and voltage of 20 kV. The samples for SEM micrographs were removed from fracture surface of the specimens for mechanical testing and placed on a steel plate by gluing a carbon tape and applying a thin gold layer of approximately 20 nm in a MED020 metallizer (BAL-TEC/MCS MULTICONTROL SYSTEM). In addition, a carbon tape was also placed on the sides of the samples, from the base to the sample surface, to electrically ground the fracture surface.

X-ray fluorescence (XRF) was performed in a Panalytical X-ray fluorescence spectrometer, model AXIOS.

Specific area analysis (SAA) using the Brunauer-Emmett-Teller (BET) method was carried out in a triStar II Instrument Plus Micromeritics Instrument. For the analysis, the rubber samples were subjected at 110 °C for 2 hours for degasification, while for sand and cement was used degassing at 200 °C for 2 hours. On the other hand, the apparent density (AD) was obtained based on the methodology of the standard practice ASTM C642 [22] by the arithmetic mean of the samples (triplicate).

3. Results and discussion

3.1. Chemical and morphological analysis of the raw materials

The results obtained by the XRF analysis of the chemical composition of the cement, rubber, and sand are presented in Table

Table 3. Chemical composition of Portland cement, rubber and sand.

Chemical component (wt%)	Portland Cement	Rubber	Sand
CaO	54.79	0.21	0.29
SiO ₂	24.72	1.95	89.6
Al ₂ O ₃	7.78	0.2	5.96
MgO	4.95	0.16	0.44
SO ₃	2.89	0.18	--
Fe ₂ O ₃	2.5	0.15	0.59
K ₂ O	0.64	0.04	2.07
Na ₂ O	0.33	--	0.73
MnO	0.56	--	--
TiO	0.5	--	0.17
P ₂ O ₅	--	0.06	0.04
Cl	--	0.01	0.02
ZnO	--	1.53	0.03
SrO	0.18	--	--
OF*	--	95.49	--

(*) Organic and sulfur fraction.

The chemical composition experimentally obtained for cement by XRF is in accordance with the established values by the Brazilian standard NBR 5735 states, determining that the composition of the cement type IS may vary depending on the chemical composition of the raw materials used and mainly on the basis of revenue, since the standard allows ranges with varying raw material dosages.

XRF analysis of the rubber waste has been performed after calcination of the material. This procedure is necessary to eliminate the organic and sulfur fraction of the material for the analysis of the other inorganic components. It can be noted that the organic and sulfur fraction of the rubber is approximately 95.49%, while the content of zinc oxide is also relatively high when compared to other oxides present in the material. Zinc is often incorporated to the rubber as zinc stearate with the purpose of leading to the

formation of surface layers on the rubber, which prevents the adhesion of the rubber with other substrates [14-17]. In the chemical analysis by XRF of the sand showed an approximate content of 90% for SiO₂, as the main constituent, and 6% for Al₂O₃, as the second major constituent.

Figure 1 shows the SEM micrographs of the cement. It is observed that the cement particles are in dimensions smaller than 25 μm and have several morphologies in which predominate smooth surfaces with sharp edges.

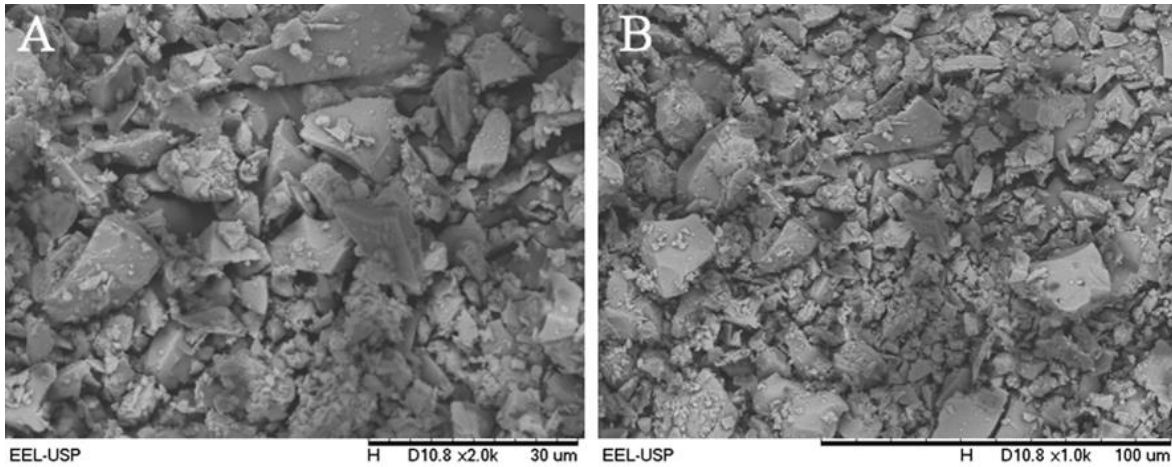


Figure 1. SEM micrograph of Portland cement: (a) 2.0 kx; (b) 1.0 kx.

The grain size ranges of the rubber waste were classified into three groups (Table 1) as coarse particles that pass through the sieve of 6-8 mesh (3.38 to 2.38 mm), medium particles of 8-10 mesh (2.38 to 1.68 mm) and fine particles of 10-20 mesh (1.68 to 0.85 mm). The rubber particle size ranges were chosen based on the characteristic aggregate size used in a traditional mortar [23]. Figure 2 shows the SEM micrographs of the rubber with fine size on the range of 0.85 to 1.68 mm.

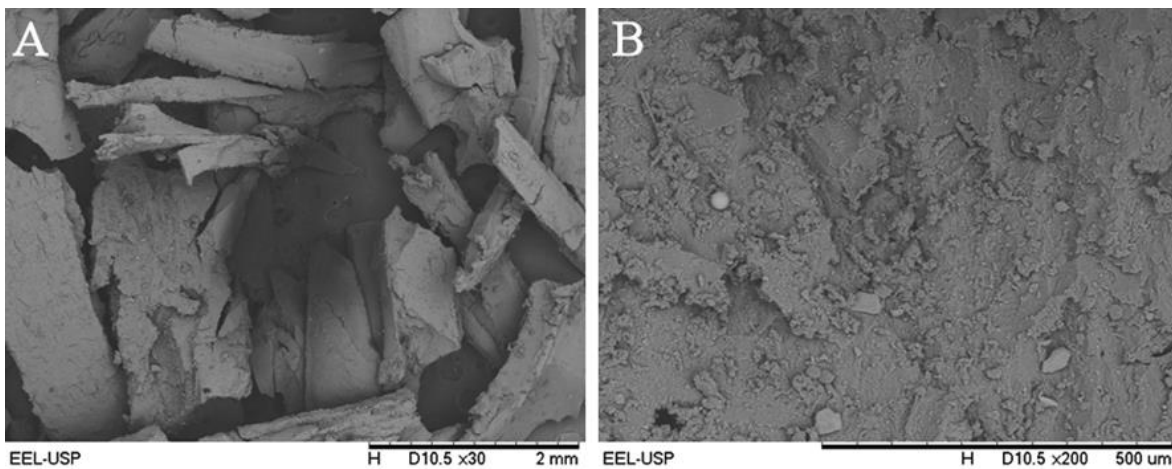


Figure 2. SEM micrograph of rubber: (a) 30x; (b) 200x.

The rubber particles present elongated shape and variable roughness due to the process of obtaining the rubber particles by scraping the tires. Additionally, it is observed that the samples have sharp edges. Table 4 presents the granulometry range of the sand which was determined by sieving.

Table 4. Sand granulometry

Particle size (μm)	Sand (wt%)
>600	Discarded
425	4%
300	66%
150	24%
<150	4%

It is observed five granulometric bands on the range of 150 to 600 μm, whose fraction with 300 μm is predominant. Particles larger than 600 μm have been discarded, while the other fractions were mixed for use as aggregate in the mortar. Specific surface area analysis (SAA) using the Brunauer-Emmett-Teller (BET) method shows for the sand a surface area of 0.18 m²/g, a pore

volume of $5.83 \times 10^{-4} \text{ cm}^3/\text{g}$ and a pore size of 129.38 \AA . For cement, the surface area is $1.06 \text{ m}^2/\text{g}$, the pore volume is $3.88 \times 10^{-3} \text{ cm}^3/\text{g}$ and the pore size is 146.74 \AA . Cement has a larger surface area than sand due to the smaller particle size, while pore volume and pore size may be related to the particle roughness. For rubber, only the particle size ranges of 1.68 to 2.38 and of 2.38 to 3.38 mm showed results of 0.18 and $0.03 \text{ m}^2/\text{g}$ for surface area, respectively. Thus, smaller particles present a larger surface area and consequent high contact surface with mortar matrix in the rubberized mortar.

3.2. Mechanical properties of the rubberized mortar

Figure 3 shows representative stress-strain curves for rubberized mortar generated by compressive tests as a function of the content and particle sizes of the rubber. Both stress and strain decrease with increasing content of rubber waste in the mortar. Thus, the incorporation of the rubber to the mortar causes notable changes in the material properties. It can be better noted through results of compressive strength and maximum compressive deformation.

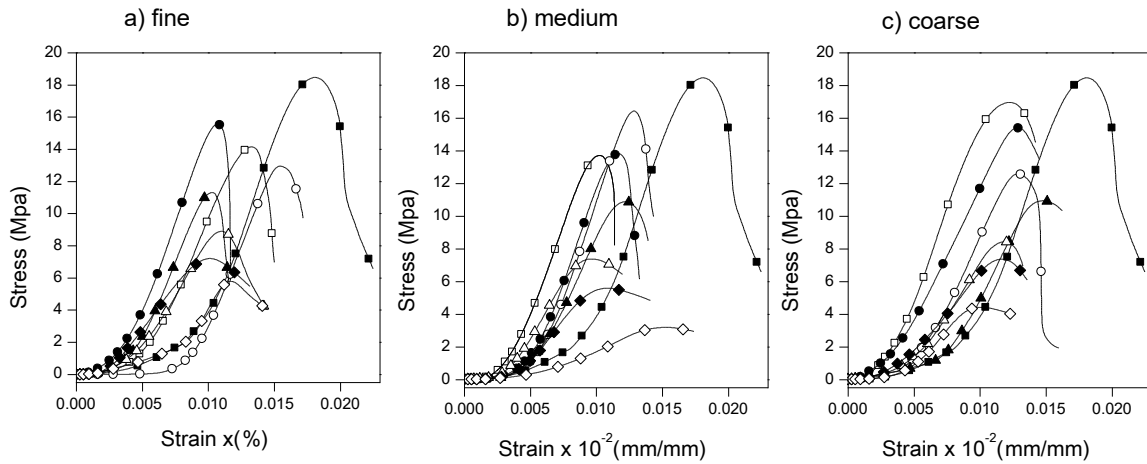


Figure 3. Stress-strain curves of compressive tests for rubberized mortar with different rubber sizes and rubber content. Rubber size: a) fine; b) medium and c) coarse. Rubber content: reference without rubber (■); 1 wt% (□); 2 wt% (●); 3 wt% (○); 4 wt% (▲); 6 wt% (△); 8 wt% (◆) and 10 wt% (◇)

The results of the compressive strength are shown in Figure 4. Rubberized mortar shows a gradual decrease in the compressive strength with increasing rubber content in the material. This decrease in compressive strength has already been widely reported by several authors [24-27]. On the other hand, there is not a significant difference in the results of the compressive strength for the three different granulometries, showing that compressive strength does not depend on the rubber granulometry.

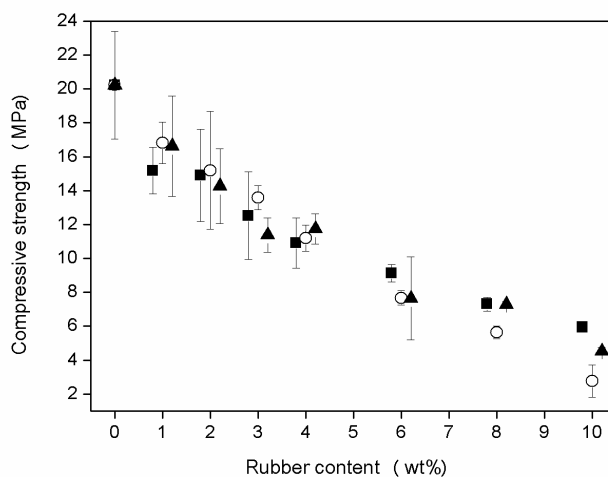


Figure 4. Compressive strength for rubberized mortar with: fine rubber particle (■); medium rubber particle (○) and coarse rubber particle (▲)

Figure 5 shows the deformation at fracture by the compressive test of the rubberized mortar. A deformation on the range of 0.9 to 2.1 mm is noted for all types of composites with different contents and granulometry of rubber. Therefore, the deformation at fracture does not depend on the presence of rubber in the mortar. The decrease in the compressive strength and the invariable compressive deformation with increasing content of the rubber in the composites can be caused because the particles of elongated

morphology generate insufficient adhesion forces in the material under compressive tensions to alter positively the compressive strength.

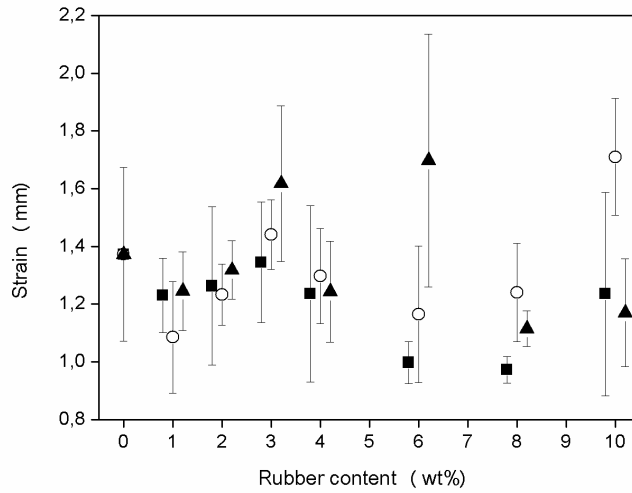


Figure 5. Maximum compressive deformation for rubberized mortar with: fine rubber particle (■); medium rubber particle (○) and coarse rubber particle (▲)

Figure 6 shows representative stress-deflection curves for rubberized mortar generated by flexural tests as a function of the content and particle size of the rubber. The mortars containing rubber at 0 to 4 wt% present the highest values of stress. However, the curves profiles change with increasing rubber content in the material. The behavior of the flexural strength of the rubberized mortar with different rubber contents is presented in Figure 7. The most important feature of the results is the preservation or increase of the flexural properties up to rubber content at around 4 wt%. At higher rubber contents, the flexural strength of the material decreases gradually. This is a plausible result since the required stress for rubber deformation is low when compared to others materials. Thus, the contribution of the rubber on the decrease in flexural strength is more significant as its content increases in the mortar. In parallel, like to the compressive test (Figure 4), it can be observed that the flexural strength is not affected by variation of the rubber granulometry indicating that in these grain sizes there is a similar mechanical property generated by them. On the other hand, it is important to note that despite the like behavior of the compressive and flexural strength of the mortar as a function of the rubber content, the absolute values for these properties are different, which corresponds to the differences in the behavior of the mortar under conditions of tension and compressive.

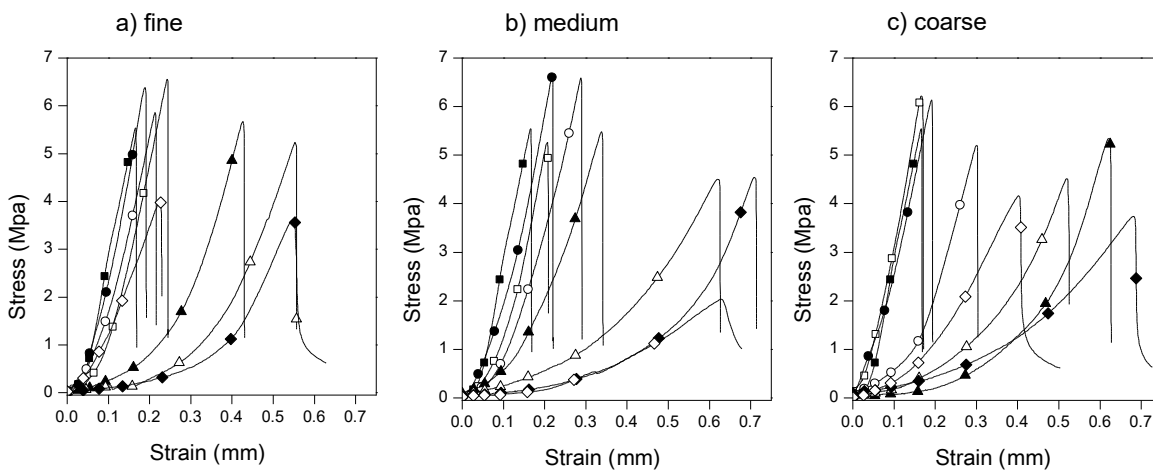


Figure 6. Stress-strain curves of flexural tests for rubberized mortar with different rubber sizes and rubber content. Rubber size: a) fine; b) medium and c) coarse. Rubber content: reference without rubber (■); 1 wt% (□); 2 wt% (●); 3 wt% (○); 4 wt% (▲); 6 wt% (△); 8 wt% (◆) and 10 wt% (◇)

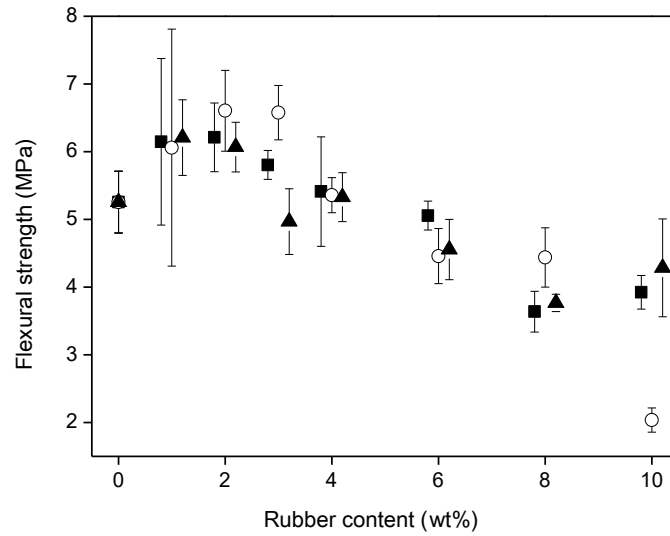


Figure 7. Flexural tensile strength for rubberized mortar with: fine rubber particle (■); medium rubber particle (○) and coarse rubber particle (▲)

Figure 8 presents the deflection generated in the flexural tests of the different compositions. It is observed that rubber contents lower than 4 wt% lead to the mortar with smaller deformations when compared to the mortar reference without rubber. However, at rubber contents higher than 4 wt% the deformations increase in relation to the reference composition. Thus, the deformations in the flexural test occur on range from about 0.15 to 0.9 mm. Additionally, an inverse behavior is observed when comparing the strength and the strain in the flexural test. Both curves present a sinusoidal behavior as a function of rubber content in the mortar. Thus, while the strength decreases for higher rubber contents, the strain proportionally increases for these values. On the other hand, this effect is inverse for lower rubber contents. The flexural resistance preservation up to around 5 wt% is possibly due to the elongated morphology particle that generates sufficient cohesive forces under tensile stresses to positively alter the flexural strength [24-27]. This feature allows advantageously selecting a processing radius depending on the requirements of the project where the material is to be employed.

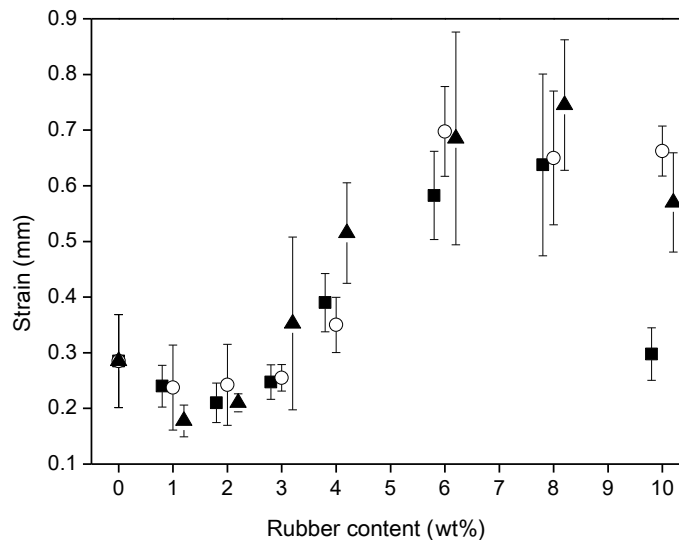


Figure 8. Maximum flexural deformation for rubberized mortar with: fine rubber particle (■); medium rubber particle (○) and coarse rubber particle (▲)

Figs. 9 and 10 show the apparent density and the volume of permeable voids, respectively. The apparent density curves show a clear decrease with the gradual increase of the rubber content independent of the kind of granulometry employed. However, when the rubberized mortars containing the same rubber content are compared, the apparent density is lower for the material prepared with the rubber of medium granulometry. For all compositions, the apparent density is in the range of 2.50 and 2.20 g/cm³. It is important to highlight the relationship between the apparent density and the mechanical properties, where a decrease

of the properties is expected with the decrease of the density of the mortar composites. In addition, the decrease in apparent density is expected considering that the density of the rubber is much lower than the density of the mortar, consequently, the gradual replacement of the mortar by the rubber will generate a gradual decrease of the apparent density.

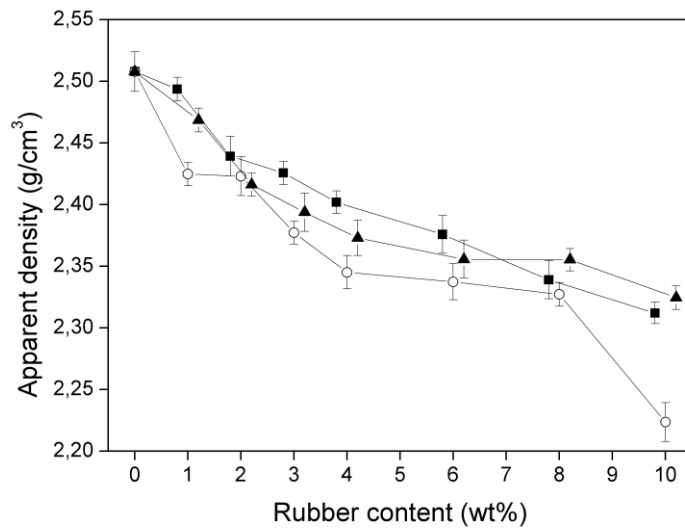


Figure 9. Apparent density for rubberized mortar with: fine rubber particle (■); medium rubber particle (○) and coarse rubber particle (▲).

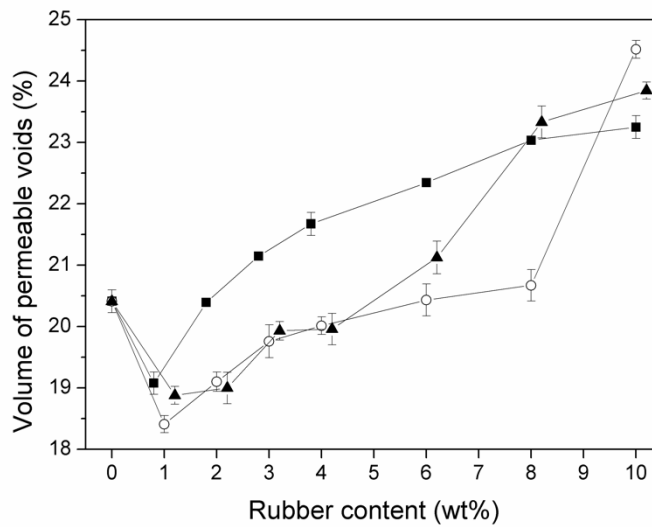


Figure 10. Volume of permeable voids for rubberized mortar with: fine rubber particle (■); medium rubber particle (○) and coarse rubber particle (▲)

On the other hand, the percentage of the volume of the interconnected voids shows an increase with the growth of the content of the rubber aggregate. The organic character of the rubber, as well as the presence of zinc stearate on the rubber surface, should cause poor adhesion between the mortar and the polymer. This poor adhesion allows the localization of air at the interface between the mortar and the rubber [11]. Consequently, the volumetric fraction of permeable air voids increases with increasing surface area of the gradually increasing rubber aggregate in the mortar composite. This can justify the increase in the volume of permeable voids and the falls in the mechanical properties of most composites. Likewise, the result of the percentage of the volume of permeable voids was confirmed using the two methods explained in ASTM C642 [22].

Figure 11 shows representative SEM micrographs of the mortar with rubber aggregate. It was possible to identify the hydrated phases as portlandite, katoite, hydrated calcium silicate, and ettringite. These hydrated phases are the main responsible of the hardening and consequently of the increase in the different types of mechanical resistances. Additionally, other phases such as aggregates of cristobalite, quartz, gypsum, and lime-free are also observed. The presence of cristobalite and quartz are usually associated with non-reactive silica from the fine aggregate fraction of the mortar. In Figure 11a of the control sample without the addition of rubber can be distinguished the different phases of the mortar, observing the fine aggregate (sand) and cementitious matrix. Figure 11b shows the micrograph obtained by SEM of the sample with 2 wt% of rubber aggregate, where

is possible to distinguish the cement phase, fine aggregate (sand) and rubber aggregate in low proportion. On the other hand, Figure 11c shows the SEM micrograph of the composite containing 10 wt% rubber. In this case, morphological characteristics similar to the composition with 2 wt% of rubber are observed.

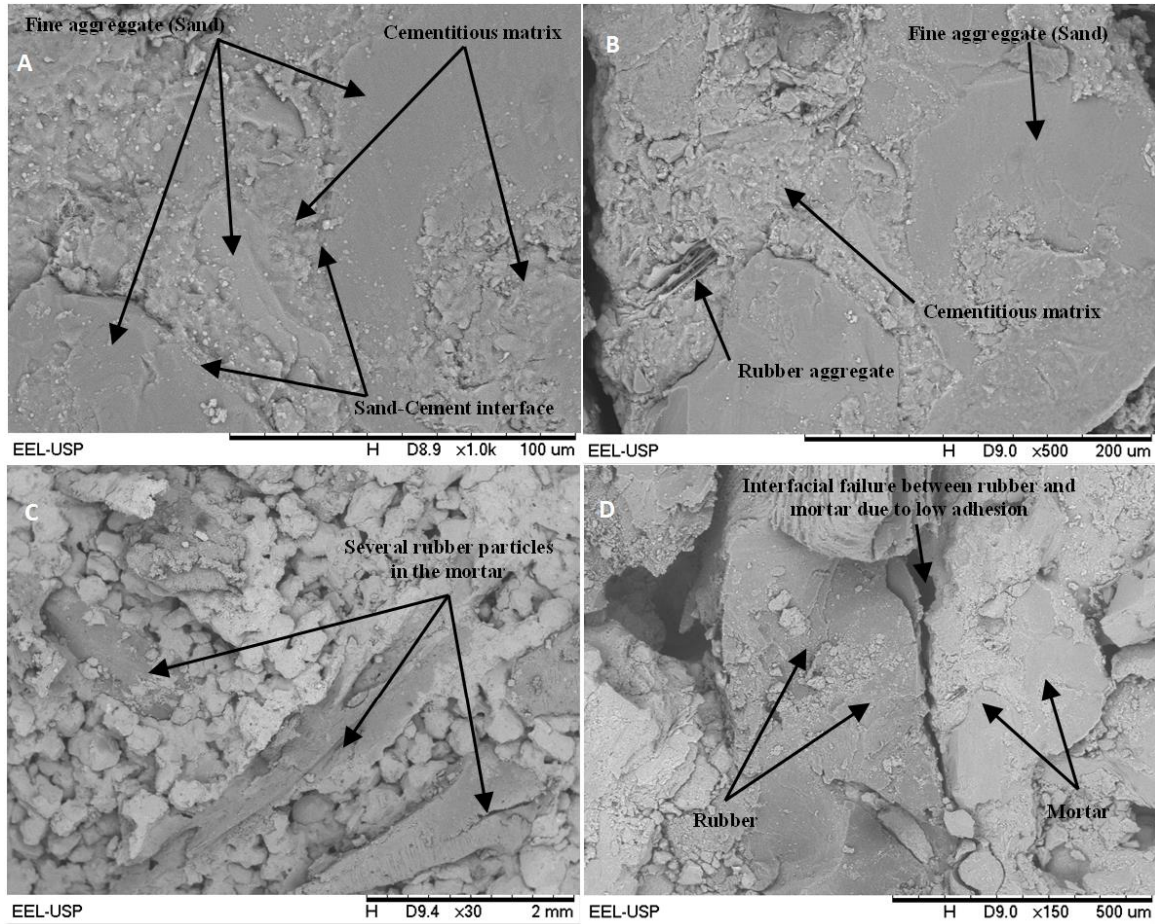


Figure 11. SEM micrograph of mortar: a) un-rubberized mortar; b) containing rubber at 2 wt%; c) containing rubber at 10 wt% and d) interfacial failure in rubberized mortar

The morphological distinction between the dispersed polymer phase and the ceramic matrix was based on the typical failure characteristics of both materials. The polymer fraction presents a high degree of deformation on torn shapes that in the case of the studied material may have this morphological attribute due to pre-treatments prior to processing or have obtained this characteristic during the treatments and/or mechanical tests of this project. On the other hand, the morphological characteristic of the surface of the mortar failure is the rough surface of the cementitious fraction or totally smooth of the fracture of the aggregate. Thus, it is possible to see in the mortar regions with pores. Likewise, energy-dispersive X-ray spectroscopy (EDS) analysis was used to distinguish the compositions of the polymer-ceramic phases of the composites.

Figure 11d shows the SEM micrograph of the mortar containing rubber at 10 wt%, focusing on the region of interfacial failure between the rubber aggregate and the mortar. Poor adhesion and void spaces can be visualized by the displacement of the rubber in the mortar. This displacement probably induces the propagation of cracks, triggering the catastrophic failure of the material. Moreover, the probability of presenting these types of faults increases by the presence of interfacial air between the mortar and the rubber aggregate and, accordingly, with the increase of the rubber content in the mortar, which justifies the decrease in the mechanical properties.

4. Conclusion

The presence of rubber particles as aggregate in mortar leads to the changes in mechanical properties of the material. Compressive strength progressively decreases as a function of the rubber content, while flexural strength increases when the rubber is incorporated to the mortar at low concentration. Flexural deformation also increases when the rubber content in the mortar is around 7 wt%. Thus, mechanical properties of the mortar are changed by inherent characteristics of the rubber, showing that there is interaction between rubber particles and ceramic matrix. However, the changes in rubberized mortar are strongly dependent of the rubber content in the mortar. On the other hand, the variation in the rubber particle size has shown insignificant changes on these properties. Rubber particle size affects properties as apparent density and volume of permeable voids, which

increase to rubberized mortar containing small rubber particles. The use of rubbers from tire waste in the mortar can be economically viable for applications where higher flexural strength is required. Thus, the production of rubberized mortar can be an interesting alternative for recycling of scrap tires.

Acknowledgements

The authors would like to thank FAPESP: Proc. 2017/05051-0, CAPES and CNPq for financial support and the Federal University of Pará for collaboration.

Data Availability Statement

All graphs and data obtained or generated during the investigation appear in the published article.

Author's Contributions:

Diego David Pinzón Moreno: Assisted the experiment's progress and helped in manuscript preparation.

Sebastião Ribeiro: Assisted the experiment's progress and helped in manuscript preparation.

Clodoaldo Saron: Drafted and wrote the manuscript, performed the experiment and result analysis.

Conflict of interest

The authors declared no potential conflicts of interest with respect to the research, authorship, and/or publication of this article.

Ethics

There are no ethical issues with the publication of this manuscript.

References

- [1] Czajczyńska, D., Krzyżyńska, R., Jouhara, H., & Spencer, N. (2017). Use of pyrolytic gas from waste tire as a fuel: A review. *Energy*, *134*, 1121–1131. <https://doi.org/10.1016/j.energy.2017.05.042>
- [2] Machin, E. B., Pedroso, D. T., & de Carvalho, J. A. (2017). Energetic valorization of waste tires. *Renewable and Sustainable Energy Reviews*, *68*, 306–315. <https://doi.org/10.1016/j.rser.2016.09.110>
- [3] Rapra, S. (2018, June 06). The Future of Tire Manufacturing to 2022. <https://www.smithersrapra.com/market-reports/tire-industry-market-reports/the-future-of-tire-manufacturing-to-2022>
- [4] Corredor-Bedoya, A., Zoppi, R., & Serpa, A. (2017). Composites of scrap tire rubber particles and adhesive mortar – Noise insulation potential. *Cement and Concrete Composites*, *82*, 45–66. <https://doi.org/10.1016/j.cemconcomp.2017.05.007>
- [5] Al-Akhras, N. M., & Smadi, M. M. (2004). Properties of tire rubber ash mortar. *Cement and Concrete Composites*, *26*(7), 821–826. <https://doi.org/10.1016/j.cemconcomp.2004.01.004>
- [6] Sienkiewicz, M., Kucinska-Lipka, J., Janik, H., & Balas, A. (2012). Progress in used tyres management in the European Union: A review. *Waste Management*, *32*(10), 1742–1751. <https://doi.org/10.1016/j.wasman.2012.05.010>
- [7] Sodupe-Ortega, E., Fraile-Garcia, E., Ferreiro-Cabello, J., & Sanz-Garcia, A. (2016). Evaluation of crumb rubber as aggregate for automated manufacturing of rubberized long hollow blocks and bricks. *Construction and Building Materials*, *106*, 305–316. <https://doi.org/10.1016/j.conbuildmat.2015.12.131>
- [8] Si, R., Guo, S., & Dai, Q. (2017). Durability performance of rubberized mortar and concrete with NaOH-Solution treated rubber particles. *Construction and Building Materials*, *153*, 496–505. <https://doi.org/10.1016/j.conbuildmat.2017.07.085>
- [9] Si, R., Guo, S., & Dai, Q. (2017b). Durability performance of rubberized mortar and concrete with NaOH-Solution treated rubber particles. *Construction and Building Materials*, *153*, 496–505. <https://doi.org/10.1016/j.conbuildmat.2017.07.085>
- [10] Shi, C., Li, Y., Zhang, J., Li, W., Chong, L., & Xie, Z. (2016). Performance enhancement of recycled concrete aggregate – A review. *Journal of Cleaner Production*, *112*, 466–472. <https://doi.org/10.1016/j.jclepro.2015.08.057>
- [11] Guo, S., Dai, Q., Si, R., Sun, X., & Lu, C. (2017). Evaluation of properties and performance of rubber-modified concrete for recycling of waste scrap tire. *Journal of Cleaner Production*, *148*, 681–689. <https://doi.org/10.1016/j.jclepro.2017.02.046>
- [12] Segre, N., Monteiro, P. J., & Sposito, G. (2002). Surface Characterization of Recycled Tire Rubber to Be Used in Cement Paste Matrix. *Journal of Colloid and Interface Science*, *248*(2), 521–523. <https://doi.org/10.1006/jcis.2002.8217>
- [13] He, L., Ma, Y., Liu, Q., & Mu, Y. (2016). Surface modification of crumb rubber and its influence on the mechanical properties of rubber-cement concrete. *Construction and Building Materials*, *120*, 403–407. <https://doi.org/10.1016/j.conbuildmat.2016.05.025>
- [14] Aziz, A., Farah, N. A., Sani, M. B., Azline, N., & Jaafar, M. S. (2017). A Comparative Study of the Behaviour of Treated and Untreated Tyre Crumb Mortar with Oil Palm Fruit Fibre Addition. *Pertanika Journal of Science & Technology*, *25*(1), 101-120.
- [15] Toutanji, H. (1996). The use of rubber tire particles in concrete to replace mineral aggregates. *Cement and Concrete Composites*, *18*(2), 135–139. [https://doi.org/10.1016/0958-9465\(95\)00010-0](https://doi.org/10.1016/0958-9465(95)00010-0)

- [16] Ganjian, E., Khorami, M., & Maghsoudi, A. A. (2009). Scrap-tyre-rubber replacement for aggregate and filler in concrete. *Construction and Building Materials*, 23(5), 1828–1836. <https://doi.org/10.1016/j.conbuildmat.2008.09.020>
- [17] Khatib, Z. K., & Bayomy, F. M. (1999). Rubberized Portland Cement Concrete. *Journal of Materials in Civil Engineering*, 11(3), 206–213. [https://doi.org/10.1061/\(asce\)0899-1561\(1999\)11:3\(206\)](https://doi.org/10.1061/(asce)0899-1561(1999)11:3(206))
- [18] Youssf, O., ElGawady, M. A., Mills, J. E., & Ma, X. (2014). An experimental investigation of crumb rubber concrete confined by fibre reinforced polymer tubes. *Construction and Building Materials*, 53, 522–532. <https://doi.org/10.1016/j.conbuildmat.2013.12.007>
- [19] ASTM C305-06. (2016). Standard practice for mechanical mixing of hydraulic cement pastes and mortars of plastic consistency. ASTM West Conshohocken, PA.
- [20] ASTM C109/C109M - 20b. (2016). Standard test method for compressive strength of hydraulic cement mortars (using 2-in. or [50-mm] cube specimens). *Annual Book of ASTM Standards*, 4.
- [21] ASTM C348. (1998) Standard test method for flexural strength of hydraulic-cement mortars. West Conshohocken, PA.
- [22] ASTM C642-06. (2008). Standard test method for density, absorption, and voids in hardened concrete. West Conshohocken, PA.
- [23] Benakli, S., Bouafia, Y., Oudjene, M., Boissière, R., & Khelil, A. (2018). A simplified and fast computational finite element model for the nonlinear load-displacement behaviour of reinforced concrete structures. *Composite Structures*, 194, 468–477. <https://doi.org/10.1016/j.compstruct.2018.03.070>
- [24] Thomas, B. S., Gupta, R. C., & Panicker, V. J. (2016). Recycling of waste tire rubber as aggregate in concrete: durability-related performance. *Journal of Cleaner Production*, 112, 504–513. <https://doi.org/10.1016/j.jclepro.2015.08.046>
- [25] Thomas, B. S., & Gupta, R. C. (2016). A comprehensive review on the applications of waste tire rubber in cement concrete. *Renewable and Sustainable Energy Reviews*, 54, 1323–1333. <https://doi.org/10.1016/j.rser.2015.10.092>
- [26] Shu, X., & Huang, B. (2014). Recycling of waste tire rubber in asphalt and portland cement concrete: An overview. *Construction and Building Materials*, 67, 217–224. <https://doi.org/10.1016/j.conbuildmat.2013.11.027>
- [27] Na, O., & Xi, Y. (2016). Mechanical and durability properties of insulation mortar with rubber powder from waste tires. *Journal of Material Cycles and Waste Management*, 19(2), 763–773. <https://doi.org/10.1007/s10163-016-0475-2>



Research Article

Influence of Marble Powder and Fly Ash on Rheological Properties and Strength of Cementitious Grouts

Hikmet Sis^{a,*} , Tufan Kıyak^b , Cenk Fenerli^c , Mehmet Genç^d 

^aFaculty of Engineering, Mining Engineering Department, Inonu University, Malatya, 44280, Turkey

^bFaculty of Engineering, Mining Engineering Department, Inonu University, Malatya, 44280, Turkey

^cHekimhan Mehmet Emin Sungur Vocational School, Malatya Turgut Ozal University, Hekimhan, Malatya, Turkey

^dHekimhan Mehmet Emin Sungur Vocational School, Malatya Turgut Ozal University Hekimhan, Malatya, Turkey

Abstract

The usability of two environmentally important waste materials in cementitious fine grout production was investigated as partial replacement materials. The study is very important in reducing carbon footprint and cost in construction industry, and improving cement properties. The influence of replacement materials on flowability and strength was investigated by rheological and compressive strength tests. With marble powder replacement, a compressive strength of 26 MPa was achieved, which was fairly above the minimum compressive strength of 14 MPa. The flowability and strength of the mixes were heavily dependent on W/C ratio and affected by type and amount of replacement materials. Increasing W/C ratio and fly ash amount increased flowability, but inversely affected strength of the grouts. On the other hand, marble powder was found to increase the strength to a large extent, but decreased the flowability. The highest increase of 24 % and the lowest increase of 5.3 % on average were achieved with 10 % fly ash and 20 % marble powder replaced mixes, respectively. The rheology data, obtained in a wide shear stress-shear rate range, were found very useful in explaining flowability as well as setting behavior (rate) of grout mixes.

Keywords: Grout; fly Ash; Marble Powder; Rheology; Compressive Strength

1. Introduction

Grout is a cementitious material, primarily composed of Portland cement and fine size aggregate combined with sufficient amount of water to produce a flowable mix [1]. Cementitious grout differs from concrete in that it contains finer aggregate and has a higher water/cement ratio. Grout is used to fill space or cavities and provide continuity between building elements and to structurally bond wall elements into a wall system [1]. ASTM C476 [2] specifies conventional cementitious grout either by proportions of the mix materials by volume or by compressive strength of hardened grout. The standard also classifies grout as either fine or coarse grout depending on the size of aggregate used. Fine grout uses only fine aggregate with a maximum size of 3/8 inches, whereas coarse grout uses both, fine and coarse aggregate with a maximum size of 1/2 inches. Among the grout ingredients, cement is the most expensive and has the largest carbon footprint due to carbon dioxide release and energy consumption during manufacturing. Reducing the amount of cement consumption in concrete (or mortar or grout) by partial replacement can reduce the carbon footprint and cost. Construction industry is searching for supplementary or partial replacement materials with the objective of reducing cost and pollution and improving the properties of cement products.

This paper was recommended for publication in revised form by Editor Orhan Canpolat

**Corresponding author/E-mail address: hikmet.sis@inonu.edu.tr. (H. Sis)*

<https://doi.org/10.29187/jscmt.2021.55>

Received 15 January 2021; Received in revised form 12 February 2021; Accepted 25 February 2021,

Available online 31 Mar 2021



Cement-based grouts with various mineral additives (such as bentonite, silica fume, fly ash, limestone powder) have been used in modern practice for various grouting applications [3]. Pozzolanic materials (e.g., fly ash and silica fume, blast furnace slag) or fine minerals (e.g., limestone powder or marble powder) contribute to certain properties of fresh and hardened concrete through hydraulic or pozzolanic activity or both. Fly ash is a cost effective cementitious material, which is utilized very commonly in manufacturing of cement or cement products (e.g., concrete, mortar or grout). When used, it reduces the amount of cement and improves flowability and spreading ability of grout [4,5]. It was also found that fly ash delays setting of grout, but could improve its compressive strength at long (e.g., 90-day or longer) aging periods [5-8].

Marble powder is a waste by-product generated as sludge in marble processing factories during sawing, honing and polishing. Marble powders constitute one of the important environmental problems all over the world as they can occupy large land areas, reduce the fertility of soil due to high alkalinity and contaminate underground water. On the other hand, they are valuable product, which can be mixed with concrete or cement to make blocks, building stones, floors and many other objects [9].

Flowability (or consistency) and strength are among the most important parameters of fresh and hardened cementitious grouts, respectively [10]. During application, flowability should be maintained so that grout can easily flow into the smallest grout spaces and around any obstructions, such as reinforcing bars, joint reinforcement, anchors, ties and small mortar protrusions. High initial flowability is needed when grout is used in congested or small spaces due to water adsorption by the masonry before and after grout placement [11]. Flowability is mainly a function of viscosity and can be increased solely by adding water, but free (unreacted) water can cause segregation, bleeding, higher shrinkage and porosity and hence causes a decrease in grout strength. Therefore, fluidity of the grout during application should be maintained, but no segregation or bleeding should be allowed.

In literature, flowability of cement grout is mainly determined by pipe flow, Marsh funnel, mini-slump and rheological tests [12,13]. There is no any specific ASTM standard on determination of flow behavior of grout, but various standards are utilized for this purpose. For example, ASTM C143 [14], which describes “standard test method for slump of hydraulic-cement concrete” is generally utilized to determine grout flowability as explained in ASTM C476 [2]. Alternatively, ASTM C939 [15] which specifies “the flow of grout for preplaced-aggregate concrete” can be also utilized to study the flowability of grouts. Rheology is a study of flow and deformation behavior of slurries and ASTM C1749 [16] specifies the measurement of rheological properties of hydraulic cementitious paste by using a rheometer. Since rheometers can test very dilute or very thick slurries, they can be used in testing fresh cementitious grout mixes, the obtained rheological parameters (e.g., apparent viscosity, yield stress, thixotropy as well as structural breakdown or build-up properties during shearing) can be related to flowability of grout. Flowability of grout mix is time dependent due to development of the bonds between the ingredients. Most of the common techniques may suffer from time-dependent physical or chemical changes, which can occur until testing the flowability [12]. Roussel and Le Roy [17] stated that for certain funnel geometries and test conditions, the flow time is a measure of flowability that can be related to the plastic viscosity and yield stress of grouts behaving as Bingham fluids. Investigations on natural hydraulic lime (NHL) grouts [18] and cement based grouts [19] exhibited a good correlation between classical flow tests and the rheological properties.

Even though the influence of incorporation of fly ash and marble powder as supplementary materials in concrete production was widely investigated, influence of these materials in fine grout production was not investigated to any great extent. In this study, the possibility of incorporating fly ash and marble powder in preparation of fine cementitious grout was investigated by partially replacing them for cement and aggregate. Interactions between the components (i.e., cement, water, aggregate, fly ash and marble powder) were inferred from rheological and strength data. The relation between flowability of freshly prepared grout and compressive strength of hardened grout was exhibited and the potential usage of fly ash and marble powder in grout mixes was assessed.

2. Materials and methods

2.1. Materials

Materials used in this study include Ordinary Portland Cement, fine aggregate, coal fly ash, marble powder and tap water. CEM I42.5R grade ordinary Portland cement manufactured by Seza Cement Factory in Baskil (Elazig, Turkey) was used in this study. Fine size aggregate (under 5 mm), produced from crushed carbonate rock, was received from local commercial aggregate production plant (Harput Concrete AŞ). The finer size fraction (under 850 µm) was separated by a standard test sieve and used in the tests. Fly ash, used as partial cement replacement material, was obtained from Soma (Turkey) coal power plant. Waste marble powder, used as partial aggregate replacement, was collected from a marble plant in Akçadağ (Malatya) region as slurry and then dried in oven at 60 °C in the laboratory.

The fly ash and dried marble powder were screened by a 300 µm standard sieve to remove any large foreign materials. Particle size distributions of aggregate, fly ash, and marble powder were measured by laser diffraction technique using Malvern Mastersizer 2000 Particle Size Analyzer (Malvern Instruments Ltd., United Kingdom) and the results are presented in Figure 1. We can see that the fine size aggregate, fly ash and marble powder have mean particle sizes of about 191, 45 and 10 µm, respectively. Blaine specific surface area and specific gravity of the components were also determined and presented in

Table 1 which shows that the fine marble powder has a much higher specific surface area of 7000 cm²/g than fine aggregate (1171 cm²/g).

Table 1. Blaine surface area and specific gravity of the grout components

Component	Blaine surface area, cm ² /g	Specific gravity, g/cm ³
Portland cement	3658	3.12
Aggregate	1171	2.80
Fly ash	4013	2.30
Marble powder	7006	2.61

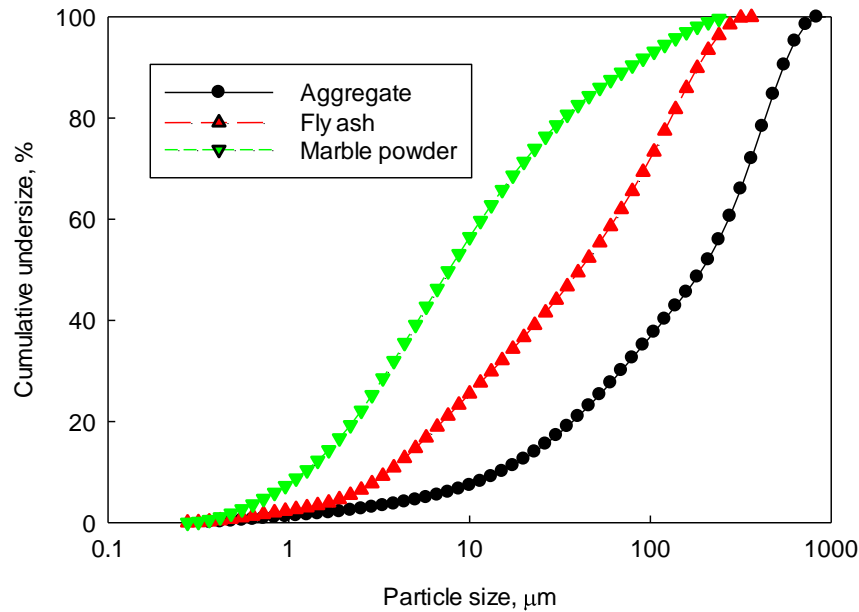


Figure 1. Particle size distribution of aggregate, fly ash and marble powder.

Table 2. XRF analysis of the grout components

Component, %	SiO ₂	Al ₂ O ₃	Fe ₂ O ₃	P ₂ O ₅	MgO	K ₂ O	CaO	SO ₃	TiO ₂
Fly ash	33.92	2.56	3.31	0.44	6.66	3.40	44.96	3.66	0.78
Marble Powder	0.42	-	0.68	-	0.34	-	98.39	-	-
Aggregate	0.83	-	1.25	-	0.23	-	97.36	-	-

The chemical and mineralogical compositions of aggregate, fly ash and marble powder were determined by XRD (Rigaku Geiger D-Max/B, Japan) and XRF (Spectro Xepos, Spectro Analytical Instruments GmbH, Germany) instruments. The XRD and XRF data are presented in Figure 2 and Table 2, respectively. As seen from Figure 2, the XRD patterns of aggregate and marble powder perfectly overlap which depict that both materials are basically calcium carbonate. XRD and XRF results also showed that the fly ash is rich for carbonates and cannot be considered as class F or class C according to ASTM C618 standard [20].

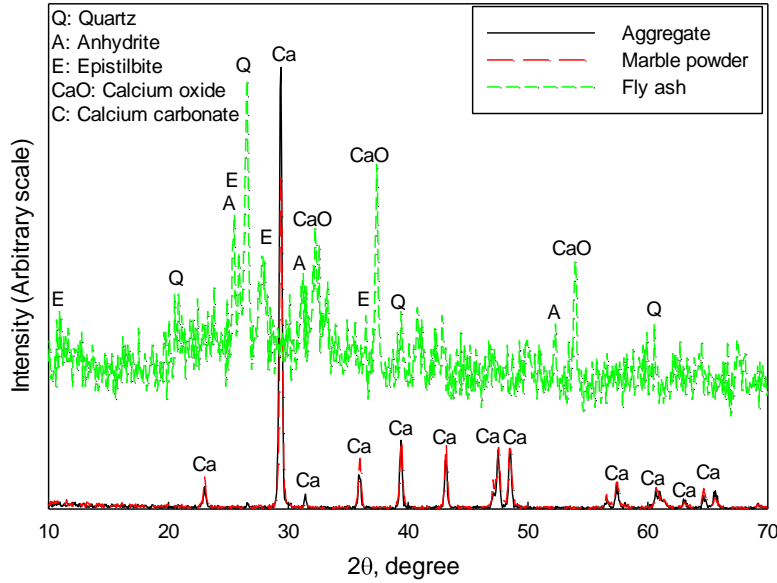


Figure 2. X-ray diffraction analysis of aggregate, fly ash and marble powder.

2.2. Methods

ASTM C476 standard [2] specifies the cement grout by proportion of ingredients or on the basis of compressive strength. The grout mixes were prepared to meet the fine cement grout specifications by proportion of ingredients. The samples were prepared at different W/C ratios in the absence and presence of fly ash and marble powder as replacing materials for cement and aggregate, respectively. Flowability of fresh mixes and strength of the hardened grout were evaluated. The influence of replacing materials was investigated at the ratios of 10 and 20 % on weight basis and the W/C ratio was varied between 1.0 and 1.4 while keeping the cement aggregate (C/AG) ratio constant at 3.0. Due to high specific surface area of the ingredients and absence of water reducing agent, high W/C ratio is required to obtain workable mixes. The mixes prepared at W/C ratio below 1.0 (at constant C/AG ratio of 3.0) were too thick (or viscous) and were not workable to carry out rheology test by the utilized set-up.

2.2.1. Rheology tests

The rheology measurement of the mixes was performed by Brookfield R/S+ rheometer from Brookfield Engineering Laboratories Inc. (MA, USA). The instrument is equipped with coaxial vane type spindle, cylindrical sample cell (cup) and a water jacket. The computer-operated rheometer utilizes the Rheo3000 software, which is capable of describing the rheological behavior of the mixes by fitting well-known rheological models to the shear stress – shear rate data. The model with the least standard error and highest correlation coefficient is recognized as the best-fit by the software. The temperature of the medium, controlled by Brookfield Circulating Bath with Digital Controller, was maintained at 20 °C for all measurements. All of the measurement variables (shear rate, temperature, measurement time etc.) were set and the spindle was placed before preparing the mix. Since the time between transferring the prepared mix into the sample cup and executing rheology test was very short (about 10 s), the mixes did not require pre-shearing. Shear rates from 0 to 600 1/s and then from 600 to 0 1/s were set as ascending and descending shear steps, respectively. The elapsed (measurement) time was kept constant as 300 s for each step.

In order to obtain reproducible results, a proper homogenization of fine ingredients is crucial. For each test, a total of 125 ml of suspension was used and the suspensions were prepared as described below;

1. All materials were precisely dry-weighted and hand mixed in a 250 ml beaker for 15 seconds by a stainless steel spatula.
2. The water is added slowly into the beaker while mixing and was mixed further for 30 seconds.
3. The mix was mixed for 60 seconds at about 600 rpm by Heidolph Hei-Torque 100 mixer equipped with a blade and immediately transferred into sample cup of the rheometer.
4. After placing the sample cup, the measurement was executed immediately at controlled shear rates (CSR).

2.2.2. Sample preparation and uniaxial compressive strength tests

Three specimens for each mix design, prepared as described above, were poured into 50 mm cubic steel molds as two layers and consolidated by hand tamping. After 24 h, the mold was removed and immediately immersed into lime containing water at 20 °C for curing. The compressive strength test was carried out on 28 and 90-day cured cubes. The tests were carried out in accordance with ASTM C109 standard [21] by using a 2000 kN capacity uniaxial compression test equipment from U-Test (Ankara, Turkey). The load was applied at 1400 N/s rate until the specimen failed. Load at the failure divided by the area of specimen gave the compressive strength of grout. Only average compressive strength value, obtained from three identical

specimen for each mix design, was reported as the result for brevity.

3. Experimental results

3.1. Rheology results

Firstly, the flow properties of mixes, prepared between 1.0 and 1.4 W/C ratios in the absence of replacing materials, were determined. Mixes were subjected to ascending and then descending shearing rates between 0–600 and 600–0 1/s and the data are presented in Figure 3(a). The mixes prepared at the same W/C ratios in the presence of replacing materials were subjected to similar rheological tests and the results are presented in Figures 3(b-g). Scales of the figures were kept constant for easy comparison. Visual inspection shows no evidence for structural breakdown of the mixes over the studied shear rate range. But, the rheograms show important differences (thixotropy) in shear stress-shear rate plots between the ascending and descending shear steps in this wide range. For given shear rates, generally higher shear stresses were obtained during descending step. It is considered that viscosity of grout is time dependent due to development of bonds and setting of mixes takes place steadily despite continuous mixing. For a given shear rate, an increase in shear stress is observed with decreasing W/C ratio and increasing marble powder content, while an opposite trend is observed with fly ash (Figures 3(a-g)). The differences were explained in term of setting rate and formation of hydration products (e.g., calcium carbo-silicate hydrate) as well as in terms of shape and filling ability of the particles. It is safe to state that low W/C ratio mixes are less flowable [10] and set faster than high W/C ratio mixes. Jiang et al. [13] investigated rheology, strength and hydration characteristics of mortars and found addition of limestone unfavorable for fluidity.

The mixes do not exhibit Newtonian (Eq. 1) behavior and deviation from Newtonian behavior increases with decreasing W/C ratio. The Rheo3000 software recognized Ostwald or power law model (Eq. 2) as the best-fit for the samples and the calculated correlation coefficient values were above 0.97. Grouts, prepared without or with replacing materials, exhibited shear thinning behavior, but the replacing materials influenced the flow differently. Bingham plastic (Eq. 3) and Herschel-Bulkley (Eq. 4) model flows, having a yield stress (τ_0) parameter in their equation, were also suggested for cement products (such as concrete, mortar, grout or paste) by some reseachers [13,19,22-24].

$$\tau = \eta \dot{\gamma} \quad (1)$$

$$\tau = K \dot{\gamma}^n \quad (2)$$

$$\tau = \tau_0 + \eta_p \dot{\gamma} \quad (3)$$

$$\tau = \tau_0 + K \dot{\gamma}^n \quad (4)$$

As rheology parameters, the constants K (in unit of Pa sn) and n (no unit) in Eq. 2 represent consistency coefficient and flow index, respectively. K is a measure of the consistency of the fluid such that, the higher the K, the more viscous the fluid. Whereas, n is a measure of the degree of non-Newtonian behavior such that, the greater the departure from unity (one), the more pronounced the non-Newtonian property [18,25,26]. The equation constants were calculated by the Rheo3000 software and presented in Table 3. As seen from the table, the consistency coefficient increases with the presence of marble powder, but decreases with fly ash. In the presence of marble powder, flow indices generally depart more from unity, which indicates more deviation from Newtonian behavior. It can be anticipated that the mixes become more viscous and less Newtonian in the presence of marble powder, whereas less viscous and more Newtonian in the presence of fly ash. Similar conclusions were achieved by several authors who investigated effect of fly ash on rheological properties of hydraulic lime grouts [10] and cement mortars [13].

The results are in-line with apparent viscosities ($\Delta\tau/\Delta\dot{\gamma}$) of the mixes calculated by the Rheo3000 software. Apparent viscosity data were evaluated as a function of shear rate, but only ascending shear step data were presented in Figure 4. It is obvious that the mixes exhibit shear thinning behavior as apparent viscosities decrease with increasing shear rate. For example, the apparent viscosities of mixes with 1.0 and 1.4 W/C ratios decreased from 1.1 Pa.s to 0.3 Pa.s and from 0.3 Pa.s to 0.08 Pa.s, respectively. Increasing W/C ratio causes the apparent viscosity of grout to decrease and flowability to increase. The mixes with lower W/C ratio kept their apparent viscosities higher in the time range of the measurement, indicating relatively faster setting of these mixes.

The incorporation of fly ash improved the flowability of the mixes, irrespective of the W/C ratio. The replacement of 10 % fly ash had negligible effect but, the improvement was more pronounced when replacement was increased to 20 %. It can be said that fly ash reduced the water requirement to achieve a certain flowability, and increased the transportability and pumpability of cement grout. Quiroga-Flores et al. [5] investigated the effect of partial replacements of fly ash and sodium-activated bentonite for Portland cement and found that fly ash improved the rheology whilst bentonite increased the thixotropy and shear thinning behavior of fresh grouts.

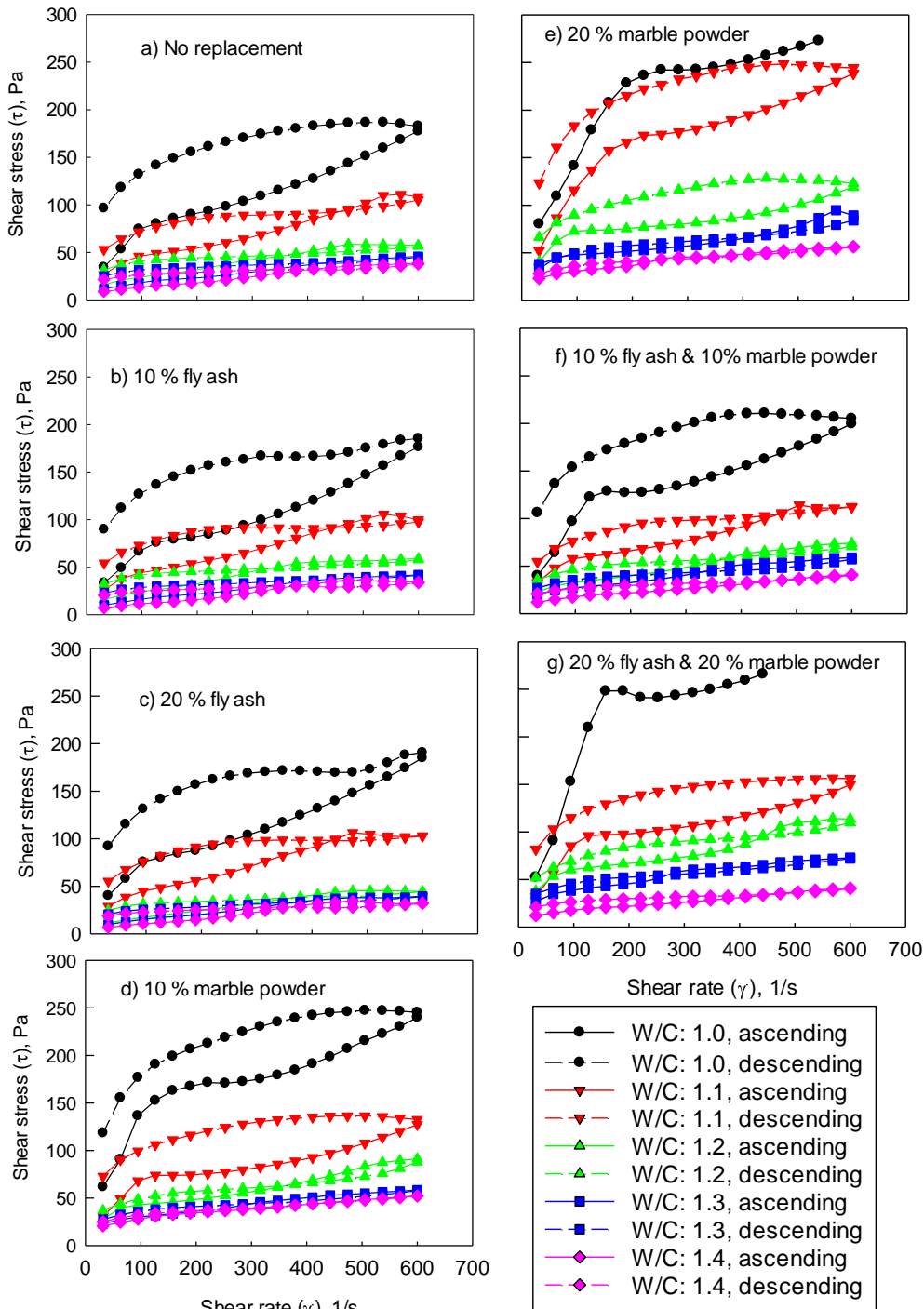


Figure 3. Shear stress-shear rate data of grout mixes prepared at different W/C ratios in the absence and presence of replacing materials.

Table 3. Mix design and replacement of fly ash and marble powder for cement and aggregate, respectively

W/C/AG ratio by weight	Replacement of fly ash or marble powder (by weight %)				Rheological parameters	
	Cement, %	Fly ash, %	Aggregate, %	Marble powder, %	Consistency coefficient, K	Flow index, n
No replacing material						
1.0/1/3	100	-	100	-	6.734	0.497
1.1/1/3	100	-	100	-	4.857	0.476
1.2/1/3	100	-	100	-	2.659	0.487
1.3/1/3	100	-	100	-	1.923	0.489
1.4/1/3	100	-	100	-	1.109	0.551
10 % Fly ash replacement						

1.0/1/3	90	10	100	-	5.699	0.515
1.1/1/3	90	10	100	-	4.827	0.475
1.2/1/3	90	10	100	-	2.563	0.498
1.3/1/3	90	10	100	-	1.527	0.518
1.4/1/3	90	10	100	-	1.000	0.557
20 % Fly ash replacement						
1.0/1/	80	20	100	-	7.719	0.476
1.1/1/3	80	20	100	-	5.136	0.473
1.2/1/3	80	20	100	-	1.636	0.526
1.3/1/3-	80	20	100	-	1.442	0.521
1.4/1/3	80	20	100	-	1.000	0.548
10 % Marble powder replacement						
1.0/1/3	100	-	90	10	23.430	0.361
1.1/1/3	100	-	90	10	9.546	0.389
1.2/1/3	100	-	90	10	7.00	0.384
1.3/1/3	100	-	90	10	6.424	0.340
1.4/1/3	100	-	90	10	2.397	0.429
20 % Marble powder replacement						
1.0/1/3	100	-	80	20	30.678	0.364
1.1/1/3	100	-	80	20	18.866	0.400
1.2/1/3	100	-	80	20	17.720	0.278
1.3/1/3	100	-	80	20	11.045	0.307
1.4/1/3	100	-	80	20	7.248	0.318
10 % Fly ash and 10 % marble powder replacement						
1.0/1/3	90	10	90	10	10.263	0.462
1.1/1/3	90	10	90	10	8.308	0.403
1.2/1/3	90	10	90	10	4.689	0.424
1.3/1/3	90	10	90	10	4.481	0.397
1.4/1/3	90	10	90	10	2.540	0.401
20 % Fly ash and 20 % marble powder replacement						
1.0/1/3	80	20	80	20	10.184	0.565
1.1/1/3	80	20	80	20	10.381	0.413
1.2/1/3	80	20	80	20	11.323	0.348
1.3/1/3	80	20	80	20	7.796	0.349
1.4/1/3	80	20	80	20	6.630	0.315

The improvement in flowability could be explained by the spherical shape of fly ash which made a lubricating effect between particles and reduced inter-particle friction that facilitated their flow. On the other hand, addition of marble powder influenced rheological properties of the mixes more than fly ash. The incorporation of very fine size marble powder significantly increased the apparent viscosity and reduced the flowability of the mixes. Rheology studies showed that the proportion of fines and hence increasing surface area of aggregates increased water demand in mortars [27] and cement pastes [23]. In other words, for a given (fixed) flowability, marble powder requires more water than aggregate due to increased surface area, and hence increased reaction with water [13]. It is also considered that, finer marble powders fill the voids between the larger aggregates, thereby make it more difficult for the solid particles to slide over each other during shearing. In binary replacements, given in Figures 4(f) and 4(g), addition of fly ash largely compensated the negative effect of marble powder on flowability.

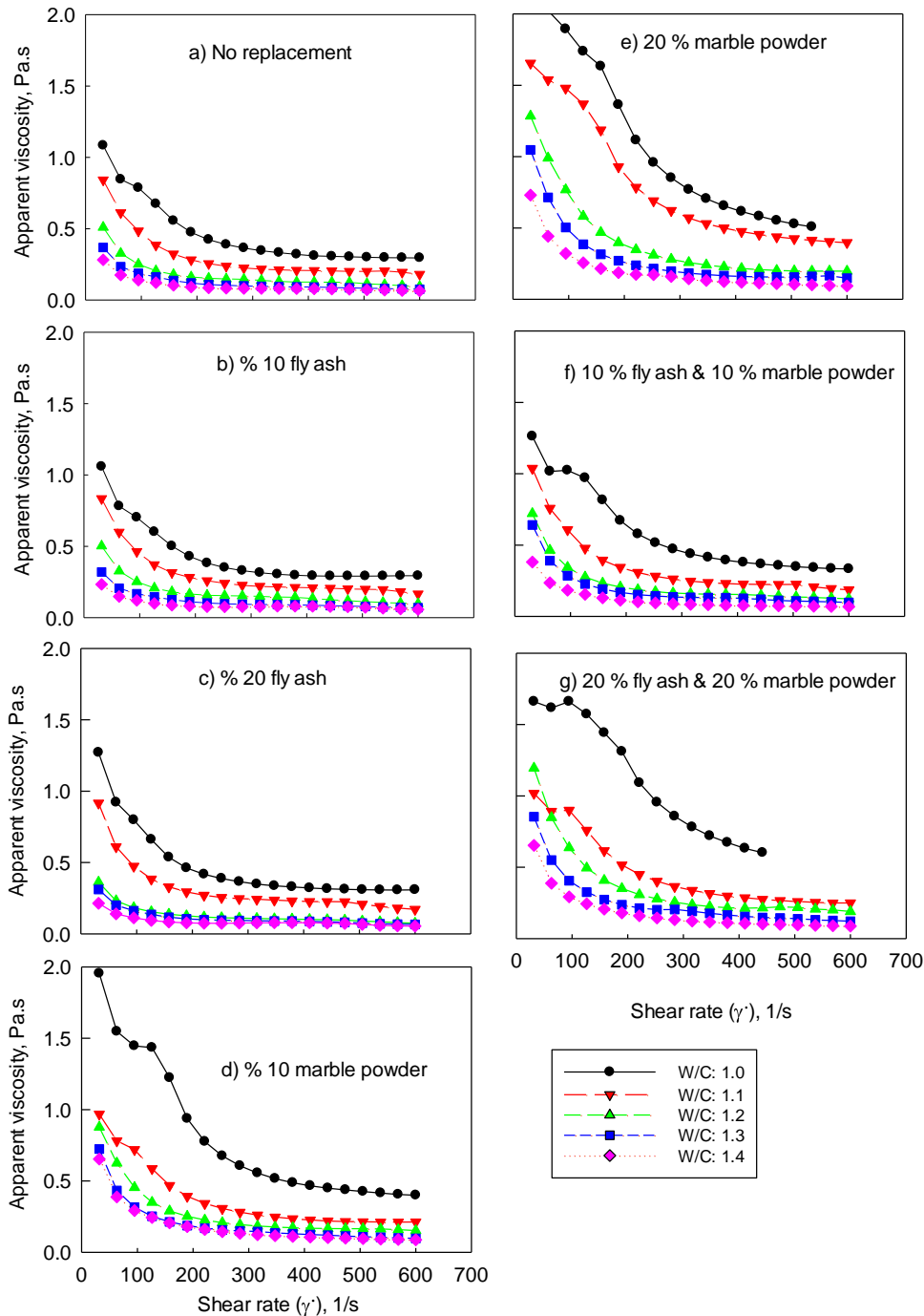


Figure 4. Apparent viscosity-shear rate of grout mixes prepared at different W/C ratio in the absence and presence of replacing materials.

3.1. Compressive strength test results

The compressive strength of grouts after 28 days and 90 days of aging was determined and the results were presented in Figure 5 and Figure 6, respectively. It can be seen from Figure 5 that the compressive strength is inversely proportional to the increase in W/C ratio, that is, the higher the W/C ratio, the lower the compressive strength. In the absence of replacement materials, the compressive strength decreased from 21.44 MPa to 7.36 MPa with increasing W/C ratio from 1.0 to 1.4. The reason for decrease in compressive strength with increasing W/C ratio is explained well in the literature. Free (unreacted) water causes pore (void) and crack generation in grout due to evaporation and can also cause bleeding and segregation during processing. ASTM C476 requires a minimum compressive strength of 2000 psi (~14 MPa) for 28 days cementitious grouts. As seen from Figure 5, grout mixes produced higher strength than specified compressive strength requirement at only 1.0 and 1.1 W/C ratios. Incorporation of 10 % and 20 % fly ash as cement replacement decreased compressive strength, respectively, by 10 % and 21 % on average at the studied W/C ratios. As known fly ash is pozzolanic material, which reacts chemically with calcium hydroxide in the presence of water to form additional calcium silicate hydrate (CSH), possessing cementitious properties. It is also known that fly ash particles increase the compactness in concrete by filling the spaces. But, the results

showed that it could not perform as well as the replaced cement, because the fly ash could not develop CSH and, due to its relatively larger size, could not fill the voids between particles as much as the cement. The lubricating effect of fly ash particle, that increased the flowability of fresh mix, can be another reason for the reduced strength. Different results found in the literature can be explained by using different types of fly ashes (i.e., class C, class F or carbonate rich) which possess different type and amount of materials. It is also considered that the hardening rate can be low for carbonate rich fly ash. The beneficial effect of fly ash could be observed when used as aggregate replacement instead of cement replacement or at curing times longer than 28 days. We can see that, fly ash replaced samples with only 1.0 W/C ratio resulted in the minimum compressive strength value of 14 MPa.

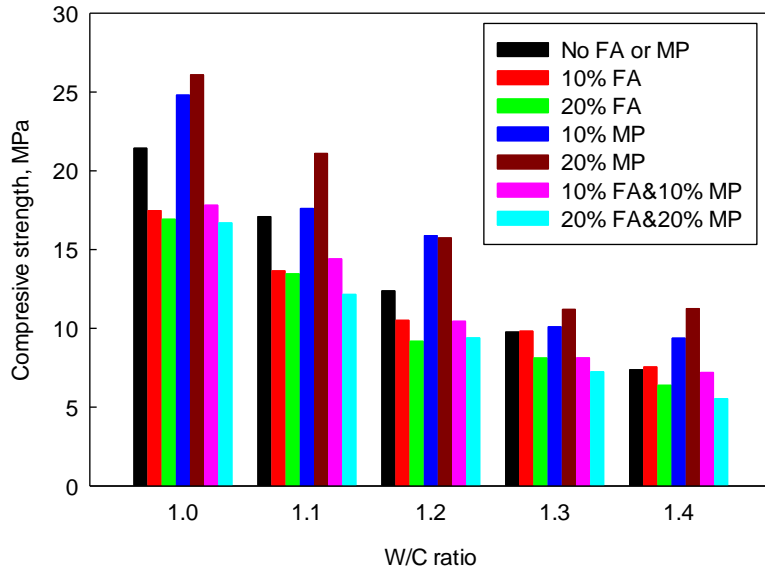


Figure 5: 28-day strength of hardened grouts prepared at different W/C ratios in the absence and presence of replacing materials

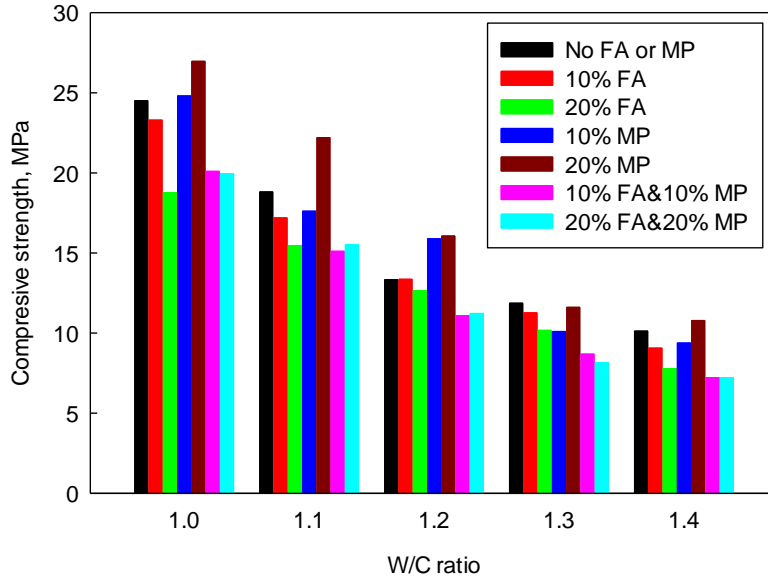


Figure 6. 90-day strength of hardened grouts prepared at different W/C ratios in the absence and presence of replacing materials

The replacement of 10 and 20 % marble powder for aggregate, respectively, increased the compressive strength about 15 and 23 % on average at the same W/C ratios. The mix prepared at 1.0 W/C ratio with 20 % marble powder replacement gained the maximum compressive strength of 26.09 MPa which is fairly above the minimum compressive strength of 14 MPa. It was possible to obtain hardened grouts with the required compressive strength from the mixes having W/C ratio not exceeding 1.2. The greater specific surface area of marble powder had a strong contribution to the mechanical strength by different ways as delineated by several investigators. Dhanalaxmi and Nirmalkumar [28] stated that additional surface area can produce more nucleation sites for cement hydration products which are responsible for grout strength. Bentz et al. [29] studied limestone and silica powder as cement replacements and showed that limestone and silica surfaces were active sites for nucleation and growth of cement hydration products, while the limestone also led to the formation of carboaluminate hydration products. It is also considered that very fine size marble powder filled voids between particles, increased the compactness and hence reduced

the porosity of hardened grout. Owing to its higher specific surface area, marble powder also reacted and consumed free water, which otherwise could cause weakness (e.g., pores, voids, cracks) upon evaporation, and at the same time prevented bleeding and segregation during processing.

The effect of W/C ratio and partial replacement materials on grout strength can be inferred from the comparable compressive strength values. Grouts without replacement material (prepared at 1.1 W/C ratio) gave a compressive strength of about 16 MPa which is comparable to 20 % marble powder replaced grout (prepared at 1.2 W/C ratio) and to 20 % fly ash replaced grout (prepared at 1.0 W/C ratio). The compressive strength of grouts at 90 days of aging was also measured and the results were exhibited in Figure 6. The strength of all mixes increased at different levels with the aging time. The highest and lowest increases in strength were achieved with 10 % fly ash (by 24 % on average) and 20 % marble powder (5.3 % on average) replaced mixes, respectively. On the other hand, the mixes prepared without replacement material gained, on average, 17 % increase in strength which became comparable to fly ash replaced mixes as seen in Figure 6. The beneficial effect of fly ash replacement on grout strength at long aging periods was affirmed by several investigators [5-8,13]. Despite the lowest increase with aging time, the highest compressive strengths were still achieved with 20 % marble powder replaced mixes having the same W/C ratio. The maximum strength of 26.97 MPa was achieved with 1.0 W/C ratio mix at this replacement. The reason for the relatively lower increase in the strength with time can be explained by the faster setting and hardening of the marble powder containing mixes, as proved by rheology measurements (Figure 3 and Figure 4). Jiang et al. [13] compared the performances of limestone powder and fly ash in mortars and found that limestone powder accelerated the hydration rate of cement, improved the hydration degree of cement and led to a denser structure due to its filling effect at early age.

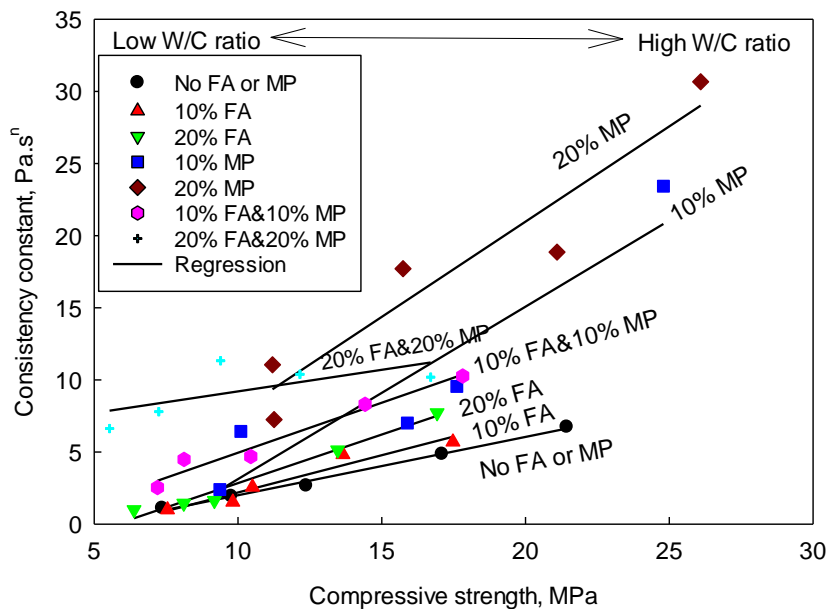


Figure 7. Variation of compressive strength of hardened grouts with consistency coefficient of fresh grout mixes

The relationship between viscosity and strength of the mix was evaluated by plotting the consistency coefficient (a measure of viscosity) versus strength data. For the sake of brevity, only 28 days strength data were plotted and presented in Figure 7. A direct relationship between viscosity and strength was mainly observed for each category. While the marble powder containing fresh mixes were generally more viscous, they became stronger after setting and hardening. It is considered that marble powder decreased flowability by increasing the viscosity, but also prevented bleeding and segregation of cement-aggregate slurries by reacting with unreacted water in the mix. When binary replacements were evaluated, it is seen that the increasing strength with marble powder was almost completely eliminated with fly ash.

4. Conclusions

Fly ash and marble powder were used in grout mix design as partial replacement materials for cement and aggregate, respectively. The following conclusions were drawn:

1. W/C ratio played the key role for grouts in attaining to certain flowability and strength and an inverse relation between flowability and strength was observed for all W/C ratios. The mixes with high W/C ratios were more flowable, but much weaker than the mixes with low W/C ratios. As an example, the compressive strength of 28-day grout decreased from 21.44 MPa to 7.36 MPa when W/C ratio increased from 1.0 to 1.4.
2. Grouts prepared without and with replacing materials exhibited shear thinning behavior, but the replacing materials influenced flow properties differently.
3. The inclusion of fly ash reduced the water demand to obtain flowable mixes but reduced the 28 days strength of grouts by

10-30 % depending on W/C ratio and fly ash amount. The lubricating effect of fly ash particles due to their spherical shape and their relatively larger sizes were considered among the reasons for enhanced flowability and reduced strength.

4. The inclusion of fine marble powder increased the viscosity of fresh and the strength of hardened grout. The highest compressive strength values were obtained with marble powder replaced grouts at given (or fixed) W/C ratios. The reason was mainly explained by filling effect of powders in the mix and increasing total surface area of the ingredients that produced more nucleation sites for cement hydration products, which are responsible for grout strength.

5. The strength of all mixes increased at different levels by increasing aging time from 28 days to 90 days. The highest increase of 24 % and the lowest increase of 5.3 % on average were achieved with 10 % fly ash and 20 % marble powder replaced mixes, respectively. The main reason was explained by the setting and hardening rate (speed) of mixes as supported by rheology results.

Acknowledgements

We acknowledge the financial support of the Scientific Research Projects Unit of Inonu University (Malatya) through project number FBA-2018-920.

Author's Contributions

Hikmet Sis: Supervised the experiment's progress, and drafted and wrote the manuscript.

Tufan Kiyak: Performed experiments, assisted in supplying experimental materials.

Cenk Fenerli: Supplied experimental materials and assisted in performing experiments.

Mehmet Genç: Supplied experimental materials and assisted in performing experiments.

Conflict of interest

The authors declared no potential conflicts of interest with respect to the research, authorship, and/or publication of this article.

Data Availability Statement

All graphs and data obtained or generated during the investigation appear in the published article.

Ethics

There are no ethical issues with the publication of this manuscript.

References

- [1] TEK 9-4A. (2005). Grout for concrete masonry National Concrete Masonry Association (NCMA), 13750 Sunrise Valley, Drive Herndon, VA.
- [2] ASTM C476. (2020). Standard specification for grout for masonry. ASTM International, West Conshohocken, PA.
- [3] Şahmaran, M., Özkan, N., Keskin, S., Uzal, B., Yaman, & Erdem, T. (2008). Evaluation of natural zeolite as a viscosity-modifying agent for cement-based grouts. *Cement and Concrete Research*, 38(7), 930–937. <https://doi.org/10.1016/j.cemconres.2008.03.007>
- [4] Sha, F., Li, S., Liu, R., Li, Z., & Zhang, Q. (2018). Experimental study on performance of cement-based grouts admixed with fly ash, bentonite, superplasticizer and water glass. *Construction and Building Materials*, 161, 282–291. <https://doi.org/10.1016/j.conbuildmat.2017.11.034>
- [5] Zobal, O., Reiterman, P., Holčapek, O., & Padevět, P. (2016). Influence of Fly Ash on Properties of Fresh and Hardened Cement Screed. *Applied Mechanics and Materials*, 825, 85–88. <https://doi.org/10.4028/www.scientific.net/amm.825.85>
- [6] Teymen, A. (2017). Effect of mineral admixture types on the grout strength of fully-grouted rockbolts. *Construction and Building Materials*, 145, 376–382. <https://doi.org/10.1016/j.conbuildmat.2017.04.046>
- [7] Ortega, J., Esteban, M., Rodríguez, R., Pastor, J., Ibanco, F., Sánchez, I., & Climent, M. (2017). Long-Term Behaviour of Fly Ash and Slag Cement Grouts for Micropiles Exposed to a Sulphate Aggressive Medium. *Materials*, 10(6), 598. <https://doi.org/10.3390/ma10060598>
- [8] Fonseca, F. S., Godfrey, R. C., & Siggard, K. (2015). Compressive strength of masonry grout containing high amounts of class F fly ash and ground granulated blast furnace slag. *Construction and Building Materials*, 94, 719–727. <https://doi.org/10.1016/j.conbuildmat.2015.07.115>
- [9] Thakur, Y. K., Kumar, M. G., & Chopra, T. G. (2014). *Effect of Marble Dust and Furnace Slag as Sand Replacement Materials on Strength Properties of Pavement Quality Concrete (PQC)* (Doctoral dissertation).
- [10] Bras, A., Henriques, F. M., & Cidade, M. (2010). Effect of environmental temperature and fly ash addition in hydraulic lime grout behaviour. *Construction and Building Materials*, 24(8), 1511–1517. <https://doi.org/10.1016/j.conbuildmat.2010.02.001>
- [11] TEK 18-8B. (2005). Grout Quality Assurance. National Concrete Masonry Association, 13750 Sunrise Valley, Drive Herndon, VA.

- [12] Mohammed, M. H., Pusch, R., Knutsson, S., & Hellström, G. (2014b). Rheological Properties of Cement-Based Grouts Determined by Different Techniques. *Engineering*, 06(05), 217–229. <https://doi.org/10.4236/eng.2014.65026>
- [13] Jiang, D., Li, X., Lv, Y., Zhou, M., He, C., Jiang, W., Liu, Z., & Li, C. (2020). Utilization of limestone powder and fly ash in blended cement: Rheology, strength and hydration characteristics. *Construction and Building Materials*, 232, 117228. <https://doi.org/10.1016/j.conbuildmat.2019.117228>
- [14] ASTM C143. (2020). Standard test method for slump of hydraulic-cement concrete. ASTM International, West Conshohocken, PA.
- [15] ASTM C939. (2016). Standard test method for flow of grout for preplaced-aggregate concrete (Flow cone method). ASTM International, West Conshohocken, PA.
- [16] ASTM C1749. (2017). Standard guide for measurement of rheological properties of hydraulic cementitious paste by using a rotational rheometer. ASTM International, West Conshohocken, PA.
- [17] Roussel, N., & Le Roy, R. (2005). The Marsh cone: a test or a rheological apparatus? *Cement and Concrete Research*, 35(5), 823–830. <https://doi.org/10.1016/j.cemconres.2004.08.019>
- [18] Baltazar, L. G., Henriques, F. M. A., & Cidade, M. T. (2015). Experimental Study and Modeling of Rheological and Mechanical Properties of NHL Grouts. *Journal of Materials in Civil Engineering*, 27(12), 04015055. [https://doi.org/10.1061/\(asce\)mt.1943-5533.0001320](https://doi.org/10.1061/(asce)mt.1943-5533.0001320)
- [19] Çınar, M., Karpuzcu, M., & Çanakçı, H. (2019). Effect of Waste Marble Powder and Fly Ash on the Rheological Characteristics of Cement Based Grout. *Civil Engineering Journal*, 5(4), 777–788. <https://doi.org/10.28991/cej-2019-03091287>
- [20] ASTM C618. (2019). Standard specification for coal fly ash and raw calcined natural pozzolan for use in concrete. ASTM International, West Conshohocken, PA.
- [21] ASTM C109. (2020). Standard test method for compressive strength of hydraulic cement mortars (using 2-in or 50 mm) cube specimens. ASTM International, West Conshohocken, PA.
- [22] Rahman, M., Wiklund, J., Kotzé, R., & Håkansson, U. (2017). Yield stress of cement grouts. *Tunnelling and Underground Space Technology*, 61, 50–60. <https://doi.org/10.1016/j.tust.2016.09.009>
- [23] Cepuritis, R., Jacobsen, S., Smeplass, S., Mørtzell, E., Wigum, B. J., & Ng, S. (2017). Influence of crushed aggregate fines with micro-proportioned particle size distributions on rheology of cement paste. *Cement and Concrete Composites*, 80, 64–79. <https://doi.org/10.1016/j.cemconcomp.2017.02.012>
- [24] Chen, J., & Kwan, A. (2012). Superfine cement for improving packing density, rheology and strength of cement paste. *Cement and Concrete Composites*, 34(1), 1–10. <https://doi.org/10.1016/j.cemconcomp.2011.09.006>
- [25] Sis, H., & Birinci, M. (2014). Wetting and rheological characteristics of hydrophobic organic pigments in water in the presence of non-ionic surfactants. *Colloids and Surfaces A: Physicochemical and Engineering Aspects*, 455, 58–66. <https://doi.org/10.1016/j.colsurfa.2014.04.042>
- [26] Kim, S. (2002). *A study of non-Newtonian viscosity and yield stress of blood in a scanning capillary-tube rheometer*, Drexel University, PA, USA, (Doctoral dissertation).
- [27] Westerholm, M., Lagerblad, B., Silfwerbrand, J., & Forssberg, E. (2008). Influence of fine aggregate characteristics on the rheological properties of mortars. *Cement and Concrete Composites*, 30(4), 274–282. <https://doi.org/10.1016/j.cemconcomp.2007.08.008>
- [28] Laxmi, C., & Kumar, D. (2015). Study on the Properties of Concrete Incorporated With Various Mineral Admixtures – Limestone Powder and Marble Powder (Review Paper). *International Journal of Innovative Research in Science, Engineering and Technology*, 04(01), 18511–18515. <https://doi.org/10.15680/ijirset.2015.0401014>
- [29] Bentz, D. P., Ferraris, C. F., Jones, S. Z., Lootens, D., & Zunino, F. (2017). Limestone and silica powder replacements for cement: Early-age performance. *Cement and Concrete Composites*, 78, 43–56. <https://doi.org/10.1016/j.cemconcomp.2017.01.001>



Review Article

Sustainable Practices in Bridge Construction

Balaji Venkateswaran^{a,*} 

^a Department of Civil Engineering, Anna University, Chennai, Tamil Nadu, India

Abstract

This paper throws light on the importance of sustainability in bridge construction projects and explains the methods to achieve sustainability in construction of bridges. The essential methods to achieve sustainability on various phases of a bridge project i.e., right from planning to maintenance of a bridge project during its service is also explained. The necessity of enacting laws to make sustainability as mandatory is outlined as conclusion.

Keywords: Bridge; Concrete; Construction; Sustainability; Life Cycle

Introduction

Sustainability is a practice in a way that the natural resources are used effectively in mining, product conversion, product production and maintenance, as a result of which, the natural resources are carried over to the future generations, without exhausting them rapidly.

Mankind has been constructing buildings, roads, bridges, railway lines, factories etc., enormously since the advent of industrial revolution. The pace of construction has always been increasing steadily around the globe, especially in fast developing countries such as India, China, Brazil, South Africa etc. Construction of structures consumes natural resources to a large extent.

The sustainability in construction could be achieved by the use of natural resources through minimising embodied energy and operational energy. Bridge construction has a substantial share in construction of infrastructure systems all over the world. Bridges are proposed over river crossing as river bridges, over and below the roads and railway lines in the form of fly overs and under bridges. Bridges are essential part of any transportation system. Bridges with spans of up to 30m constitute the vast majority of road infrastructure bridges in service across the world [2]. Higher is the construction area of a bridge project, higher is the consumption of natural resources. Hence astute planning is required for the construction of a bridge project in order to achieve sustainability.

This paper was recommended for publication in revised form by Editor Mukhallad Al-mashhadani

**Corresponding author/E-mail address: bakrkaku@gmail.com (B. Venkateswaran)*

<https://doi.org/10.29187/jscmt.2021.56>

Received 22 February 2020; Received in revised form 28 August 2021; Accepted 30 August 2020,

Available online 31 March 2021



Sustainability Thinking in Bridge Construction

Sustainability in bridge construction could be achieved through planning, design, construction and maintenance of a bridge [5]. Sustainability in a bridge project could be viewed from achieving minimum embodied and operational energy during its construction and maintenance [2].

2.1 Embodied Energy

Embodied energy in a bridge project results from the use of materials for the construction of a bridge, i.e., energy consumed by the materials in mining, stacking, sorting, conversion in to other products, transportation of the converted product, their storage or laying the finished products in their intended place.

2.2. Operational Energy

Operational energy is the energy consumed in operation and maintenance of a bridge structure, during its entire life span. In order to achieve sustainability in construction of bridges, their embodied energy and operational energy should be minimum.

2.3 Sustainability in Planning a Bridge Project

Planning for a bridge project involves selecting a suitable location for the bridge in terms of minimum length of the proposed bridge, selecting an economic span for the bridge and selection of suitable superstructure forms such as girder bridge, arch bridge, suspension bridge, cable stayed bridge etc. The form of sub structure to be selected for a bridge project depends upon its height and the span proposed. The foundation for a bridge project depends upon the soil profile at the project location based on which the foundation shall be of pile, raft and open spread footing.

Selection of particular location for a bridge project, its superstructure, sub structure and foundation contribute a lot in achieving sustainability. A perspective that longer the bridge, higher is the material consumption for construction and the maintenance shall also be considered. The selection of site for a bridge construction shall also be made in such a way that neither its approach nor its span is located on the wet irrigation fields, forest area, lakes, tanks, reservoirs, zoological conservatories etc., in such a way that micro climate of the region, habitats of the region are not affected and water retention area of the water bodies are not shrunk in any way. The bridge should also be planned in such a way that livelihood of people living in the area is not affected in any way. Planning should also be in such a way that the natural formations such as hills, mountain ranges are not affected.

New bridge in lieu of the existing bridge may be planned if it is absolutely essential to reconstruct the bridge otherwise the existing bridge may be strengthened to achieve extension of its service life.

2.4 Sustainability in Design of Bridges

The design components of a bridge structure must be meticulously done in such a way the structure integrates well in to the atmosphere. The structure should not be a loner in the surroundings. The bridge span, material for construction of the bridge, location of piers and abutments, construction of retaining walls to retain the approaches or river bunds, river bed protective works are all designed in such a way that they consume minimum natural resources and deployment of machineries for their construction.

Design of bridges should be in such a way that they need less repair and restoration effort during their entire service life. Possibility of use of locally available materials and the use of recycled materials should also be explored in the design stage. The use of alternate and appropriate technologies should also be explored.

2.5 Analysis for Life Cycle Analysis of a Bridge Structure

Life Cycle Analysis (LCA) [1,2] is a method to evaluate all the aspects connected with bridge construction and its associated environmental impacts during its entire service life including its material procurement, their transportation, use, and their final disposal in such a way that the net embodied energy, operational energy and the emission of carbon dioxide (CO₂) is minimum. As in Figure 1. [4] the LCA also aims to achieve balance in economics i.e., the cost incurred in construction and

maintenance of a bridge structure, maintaining the environment of the locality (The minimum change in micro and macro climate of the area and the minimum disturbance to habitat of the region) and the social impacts due to construction. (The impact on the livelihood of the locality should be minimum, rehabilitation and resettlement should also be kept minimum).

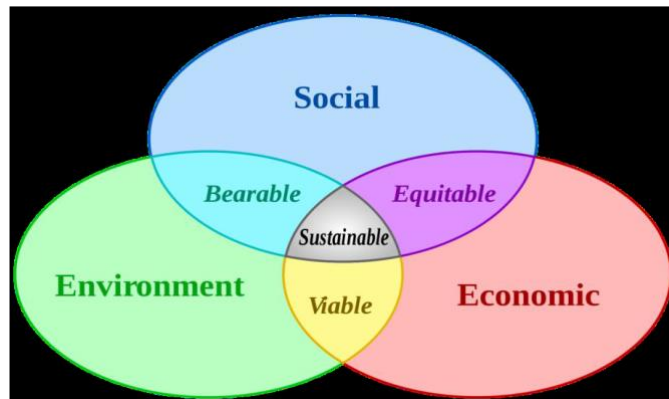


Figure 1. Sustainable Parameters

Thus, a sustainable bridge project, as shown in Figure 1. [4] shall be economically viable, environmentally justifiable or bearable and must create an equitable social environment.

In any bridge project, common materials for use in their construction are concrete, steel and composites of steel and concrete. Table 1. Shows the embodied energy and CO₂ emissions on different forms of bridge structures using different materials for their construction [2]. It can be inferred from the above table that considering various bridge forms, bridge constructed using concrete consumes less energy and emit minimum CO₂ emission.

Table 1. Bridge forms and embodied energy consumption

Energy	Structural Form	Embodied Energy during construction(GJ/m ²)			CO ₂ Emissions during construction(Kg/m ²)		
		steel	Concrete	Composite	steel	Concrete	Composite
Minimum	Viaduct	17.6	15.7/16.6	22.1	1464	1445/1446	1453
	Girder	30.9	23.6	29.1	2513	2132	2440
	Arch	49.5	34.3	48.8	3952	3536	4036
	Cable-stay	40.3	21.1/22.1	37.7	3406	3242	3372
Average	Viaduct	23.3	21.1/22.1	22.1	1719	1710/1863	1702
	Girder	39.3	30.6	37	2810	2457	2750
	Arch	61.9	49.1	60.8	4326	4005	4459
	Cable-stay	50.6	43.9	47.7	3822	3726	3830
Maximum	Viaduct	30.8	28.1/28.6	29.2	1891	1912/2066	1893
	Girder	49.3	39.1	46.6	3045	2718	2998
	Arch	75.6	60.9	74.4	4637	4410	4820
	Cable-stay	62.6	54.8	69.3	4174	4140	4244

2.6 Sustainability in Construction of Concrete Bridges

Sustainability in construction could be achieved in many ways. The chief among them are.

- Procurement of materials

- Storing/Stacking of materials
- Testing of materials
- Use of materials for construction
- Construction techniques
- Project management
- Maintenance of the structural components

2.6.1 Procurement of Materials

The essential procurements for a bridge structure consist of:

- Cement
- Steel
- Coarse aggregates and fine aggregates
- Earth for formation of approaches

Cement of required grade should be produced in bulk rather than in loose quantities. This reduces the cost of fuel used for transportation and in turn reduces operation energy. The procured cement should be stored in such way that the cement should be used till the end of the construction without any loss in the property of cement.

Steel of required quality and quantity should be procured well in advance before the commencement of RCC construction. They should be cut in such a way that wastages are minimum.

Coarse and fine aggregates should be sourced nearer to the site and the use of locally available materials should be encouraged. Earth of required quality should be sourced nearer to the site rather than conveyed from a distance.

2.6.2 Stacking

Stacking of construction materials should be done nearer to the site. In the case of concrete, the raw materials should be stored in such a way that batching of concrete is done quickly, without any need for longer conveyance for mixing and placing of concrete.

2.5.3 Testing of materials

Testing and certification of materials should be carried at the source itself rather than at the site. This obviates the necessity for return transportation, if there is any need for rejection of materials.

2.5.4 Construction Techniques

Construction of the bridge components should be planned in such a way that each of them is carried out in minimum possible time by employing suitable construction techniques. Time delay and cost overrun are indirectly related to sustainable construction. The form work and scaffolding materials should be of such a quality so that the finished concrete is within the tolerance limits and the form work materials can be reused to the maximum extent as possible, without any loss in their integrity and the finished concrete is not out of dimension.

2.5.5 Project Management

Project management contributes to the sustainable goals by means of effective utilisation of resources and manpower. Scientific implementation of a bridge project by means of employing construction management principles shall be explored. The use of Project Evaluation and Review Technique (PERT), Critical Path Method (CPM)) and the project management software tools such as PRIMAVERA for large projects, shall also be considered.

The concept of Building Information modelling (BIM) shall also be considered for the bridges as various stages of a bridge project are integrated in to a single model i.e., right from planning, design, and estimation to the execution. This proves to be cost effective and contributes to sustainability in a huge way.

2.5.6 Maintenance of the Structural Components

The maintenance of a bridge structure contributes a lot to the sustainability. Maintenance includes adhering to the quality control norms during construction, particularly in areas with severe exposure conditions. In order to meet norms for severe exposure conditions, larger cover for concrete components is prescribed, treatments of steel using epoxy coatings, use of Sulphate resistant cement for foundation are also prescribed.

Apart from the above, routine inspection and testing are also needed to ensure that the bridge components complete their service life satisfactorily. Undertaking immediate repair of any faulty components also ensures the structural integrity of the bridge structure. The maintenance of the bridge components in a routine manner also makes the structure to live beyond their service life. Extending the life of a bridge structure also make them sustainable.

Conclusion

The bridges are vital infrastructures of any economy. Wherever the economy is growing, the bridge infrastructure also increases. As a result, sustainability has become an important factor to look in to so that the bridge structures are not only sustainable but are also cost effective. This results in substantial saving in economy, particularly in developing countries. Thus, sustainability should be an integral part of an estimate for any bridge project. Construction rules globally should be enacted so that the sustainability is given due consideration for any bridge project.

Acknowledgement

The author wishes to acknowledge all researchers, scientist, planners, builders, government agencies, interest groups who work to achieve sustainability a way of practice and thus to save our planet from imminent catastrophe.

Conflict of interest

The author declared no potential conflicts of interest with respect to the research, authorship, and/or publication of this article.

Ethics

There are no ethical issues with the publication of this manuscript.

References

- [1] Ahlborn, T., (2020, January 10). Sustainability For the Concrete Bridge Engineering Community, ASPIRE Magazine, Precast concrete Institute, Winter Issue. http://aspirebridge.com/magazine/2008Winter/ASPIRE_win08.pdf
- [2] Buffenbarger, J., (2020, January 10). Sustainable Bridges and Infrastructure (Part II), U.S. Department of Federal Highway Administration, Issue 77, <http://www.concretebridgeviews.com>
- [3] Long, A. E., Venables R. K., Ferguson J. D., (2020, January 10) . Sustainable bridge construction through innovative advances, Queen's University, Belfast, U.K., Accessed on line 2020, <http://www.irbnet.de/daten/iconda/CIB11831.pdf>
- [4] Myint, L. (2019). LRFD Bridge design manual ,Sustainable bridge design, IOWA Department of Transportation Des Moines, Iowa, USA.
- [5] Whittmore, D., (2020, January 10). Sustainable structures for the bridge engineer, Structure Magazine, Accessed on line 2020 <http://www.concretebridgeviews.com>



Research Article

Investigation of Mechanical and Permeability Properties of Fiber Mortars

Veysel Akyüncü^{a,*} 

^aDepartment of Civil Engineering, Corlu, Tekirdag Namik Kemal University, Tekirdag, Turkey, 59860

Abstract

Concrete is a brittle material which has a higher compressive strength compared to its tensile strength. Steel, glass or polymer fibers are usually added to concrete in order to improve the ductility under mechanical loads. One of the most important factors taken into consideration in producing a durable concrete is by imperviousness concrete. In this study, the mechanical and permeability properties of fiber reinforced mortars were investigated. For this purpose, in addition to the reference, 0.1%, 0.2% by volume, glass fiber reinforced and 1.15% and 2% impermeability admix incorporated series were prepared. The effective water/cement ratio of all produced mortar samples was determined to be 0.5. The workability, ultrasonic pulse velocity (UPV), flexural strength, compressive strength, splitting tensile strength, determination of water penetration depth under pressure were determined in all series. According to the test results, as the glass fiber ratio increased, the water penetration depth decreased by 15% compared to the reference. In the series where 0.2% glass fiber was used, there was a 20% increase compared to the reference in terms of splitting tensile strength. In addition, there is an increase in splitting tensile strength in series produced using glass fiber and impermeability additive.

Keywords: Mechanical Properties; Compressive Strength; Fiber Glass; Splitting Tensile Strength; Permeability

1. Introduction

Concrete; It is a three-phase heterogeneous material consisting of aggregate, cement paste and the interface of these two components. Aggregate cement paste interface is known as the weakest link in concrete. The formation of cracks at the aggregate-paste interfaces plays an important role in the inelastic behavior of concrete. Studies where microcracks start in the coarse aggregate and the mortar surrounding it and crack propagation takes place at the interface point to the importance of this phase of concrete [1,2]. For this reason, the improvement in mortar properties makes a very important contribution to the strength and durability properties of concrete [3]. Glass, steel and polypropylene fibers, which have a certain length / diameter (slender ratio) ratio, are widely used in order to improve concrete properties positively. Homogeneously dispersed fibers prevent the cracks that occur in the concrete and contribute positively to the strength and durability of the concrete by slowing the progress of the cracks in the concrete. In addition, the energy absorption capacity of concrete can be increased by using fiber in concrete [4].

Today, steel and polymer fibers are widely used in fiber concrete production. However, in recent studies, glass, basalt etc. are used as an alternative to these fibers. There is also an increase in studies with fibers [5-7]. Some features that fibers bring to the fresh mixture; It can be expressed as shrinkage, induced plastic crack formation, segregation, permeability and consistency reduction. Fibers increase the toughness and impact toughness of the hardened mixture, surface wear resistance, fatigue resistance, chemical resistance, fragmentation resistance and freeze-thaw cycle resistance [8-10]. In spite of the great interest in

This paper was recommended for publication in revised form by Editor Xiaojian Gao

** Corresponding author/E-mail address: vakyuncu@nku.edu.tr. (V. Akyüncü)*

<https://doi.org/10.29187/jscmt.2021.57>

Received 27 February, 2021; Received in revised form 17 March, 2021; Accepted 20 March, 2021,

Available online 31 March 2021



polymer composites usage in construction, concrete is still the main building material. For this material, there has been a significant amount of research from involvement of modifications to the use of glass fiber as well [11-13]. Compared to non-modified concrete, glass fiber modified concrete showed better results in mechanical performance and properties as reported by Sanjeev and Sai Nitesh [14]. The increase in compressive, splitting tensile strength, and flexural strength in combination with decrease in slump fall were noticed.

Durability and permeability in concrete are two closely related events. Permeability of concrete; pressurized water is realized by capillary water absorption and steam. If the necessary precautions are not taken in terms of impermeability, this three permeability in concrete reach high values in the same direction and negatively, and this leads to problems in terms of durability. It is extremely important that the concrete to be used in areas exposed to water or moisture is suitable for environmental conditions. Although insulation materials are used in such areas, the risk of exposure to moisture and corrosion is high. The effect of corrosion on structures is devastating. Impermeable concretes protect steel reinforcement against corrosion and external influences [15,16].

In this study, the effect of glass fiber and impermeability additives used in different proportions by keeping sand, water and cement constant on mechanical and permeability properties was investigated. It is aimed to 0.1%, 0.2% by volume, glass fiber reinforced and 1.15% and 2% impermeability admix incorporated series were prepared. This objective is supported by various tests such as workability, UPV, flexural strength, compressive strength, splitting tensile strength, determination of water penetration depth under pressure.

2. Experimental Study

2.1. Materials and Mix Proportions

Powdered crystalline impermeability additive with a density of 1.04 g/cm³, 24 mm glass fiber, standard Rilem sand and CEM I 42.5 R cement were used. Water / binder ratio was chosen as 0.5 in the productions. In addition to the reference, 0.1%, 0.2% glass fiber ratio, 1.15% and 2% impermeability additives, a total of 9 batches production were made, with fibrous and impermeability additives. Fiber ratios were used by volume, and impermeability additive was used as percentage of cement by weight. Mortars were cured in 20 ± 1 ° C lime saturated water in accordance with the TS EN 196-1 [17] standard and subjected to mechanical tests at the of 28 days. Properties of cement and glass fiber used in mortar production are given in Tables 1 and 2. Standard CEN reference sand was used as aggregate. Table 3 shows the properties of the CEN reference sand.

Table 1. Chemical, physical and mechanical properties of cement

Components (%)	CEM I 42.5 R
CaO	64.12
SiO ₂	20.23
Al ₂ O ₃	5.09
Fe ₂ O ₃	3.34
MgO	1.15
SO ₃	2.98
Na ₂ O/K ₂ O	0.1/0.74
Cl ⁻	0.0324
Loss of ignition	2.45
Insoluble residue	0.78
Physical and mechanical properties of cement	
Specific gravity	3.06
Specific surface (cm ² /g)	3520
Initial setting time (min)	185
Final setting time (min)	250
7 days (MPa)	46.9
28 days (MPa)	59.9

Table 2. Properties of glass fiber

Length (mm)	Density (g/cm ³)	Tensile strength (MPa)	Modulus of elasticity (MPa)	Diameter (μm)
24	2.6	3400	77000	14

Table 3. Particle size distribution of CEN standard sand

Sieve size (mm)	2.00	1.60	1.00	0.50	0.16	0.08
Aggregate remaining in the sieve (%)	0	7 ± 5	33 ± 5	67 ± 5	87 ± 5	99 ± 1

2.2. Sample Preparation, Curing and Testing Procedure

Production of mortar samples was carried out in Tekirdağ Namık Kemal University Çorlu Engineering Faculty Building Materials Laboratory. 27 different mixes were prepared. A total of 243 prism and 27 cube mortar samples, were cast. Table 4 gives the details on how the samples were coded.

Table 4. Sample coding

Sample code	Definition
REF-%0-%0	Reference specimens cured in water until testing day
L24-%0,1-%0	24 mm fiber length -% 0,1 glass fiber ratio -% 0 admixture ratio
L24-%0,2-%0	24 mm fiber length -% 0,2 glass fiber ratio -% 0 admixture ratio
L24-%0-%1,15	24 mm fiber length -% 0 glass fiber ratio -% 1,15 admixture ratio
L24-%0,1-%1,15	24 mm fiber length -% 0,1 glass fiber ratio -% 1,15 admixture ratio
L24-%0,2-%1,15	24 mm fiber length -% 0,2 glass fiber ratio -% 1,15 admixture ratio
L24-%0-%2	24 mm fiber length -% 0 glass fiber ratio -% 2 admixture ratio
L24-%0,1-%2	24 mm fiber length -% 0,1 glass fiber ratio -% 2 admixture ratio
L24-%0,2-%2	24 mm fiber length -% 0,2 glass fiber ratio -% 2 admixture ratio

3. Results and Discussion

3.1. Mechanical properties

Flow diameter, UPV, flexural strength, compressive strength, splitting tensile strength, permeability test results are given in Table 5.

Table 5. Mechanical and physical properties of the mixtures

Mixtures	Flow diameter (mm)	UPV (mm/μs)	Flexural strength (MPa)	Compressive strength (MPa)	Splitting Tensile Strength (MPa)	Pressure water Processing Depth (mm)
REF-%0-%0	17.92	4.48	11.48	41.37	3.60	12.33
L24-%0,1-%0	15.98	4.45	11.45	39.83	4.07	11.66
L24-%0,2-%0	14.67	4.43	11.69	39.79	4.35	10.67
L24-%0-%1,15	16.30	4.51	11.14	34.48	5.50	12.00
L24-%0,1-%1,15	14.92	4.53	12.16	27.34	6.07	15.00
L24-%0,2-%1,15	13.83	4.50	11.86	27.31	5.89	11.00
L24-%0-%2	15.18	4.48	11.21	34.43	5.48	17.33
L24-%0,1-%2	13.50	4.37	9.92	14.80	-	-
L24-%0,2-%2	13.28	4.48	11.24	14.90	-	-

3.1.1. Workability

The flow diameters of the mortar samples are shown in Figure 1. The flow diameters vary between 13-18 cm. When Figure 1. is examined, the spreading diameter decreased as the fiber ratio and impermeability contribution increased. Karahan and Atis [18] and Shekarchi et.al [19] reported that inclusion of polypropylene fiber reduced workability and increase in fiber content caused additional reductions in workability.

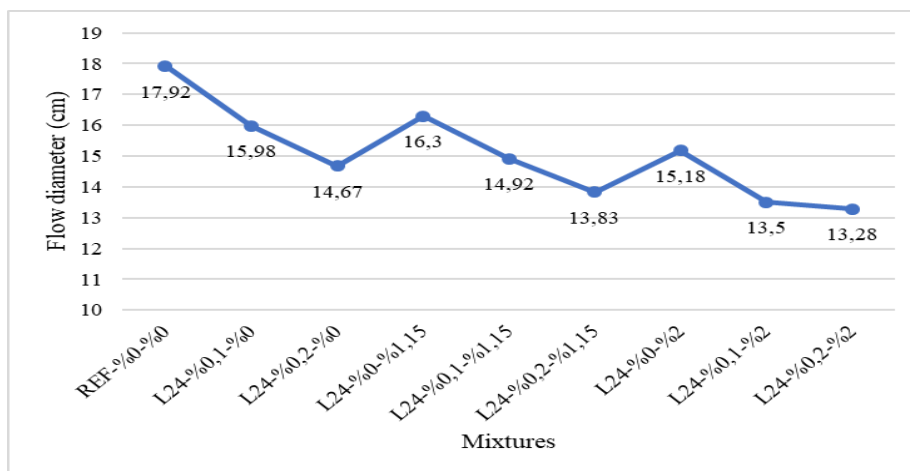


Figure 1. Results of flow diameter

3.1.2. Compressive strength and Flexural strength

The graph of the change in the tensile strength and compression strength in bending is given in Figure 2. At the reference with the highest compressive strength, 41.37 MPa was the lowest value, and 14.90 MPa in the series L24- 0.1% -2%. As the fiber ratio and water impermeability additives increased in L24- 0.1% -2% and L24-0.2% -2% series, a decrease in compressive strength was observed. Similar results were reported by several researchers [20-21]. Flexural strength gave close values in all series. Bhargava et al. [22] stated that the 4% decrease in compressive strength, 14% decrease in splitting tensile strength, and 13% in flexural strength for concrete modified with glass fibers was obtained.

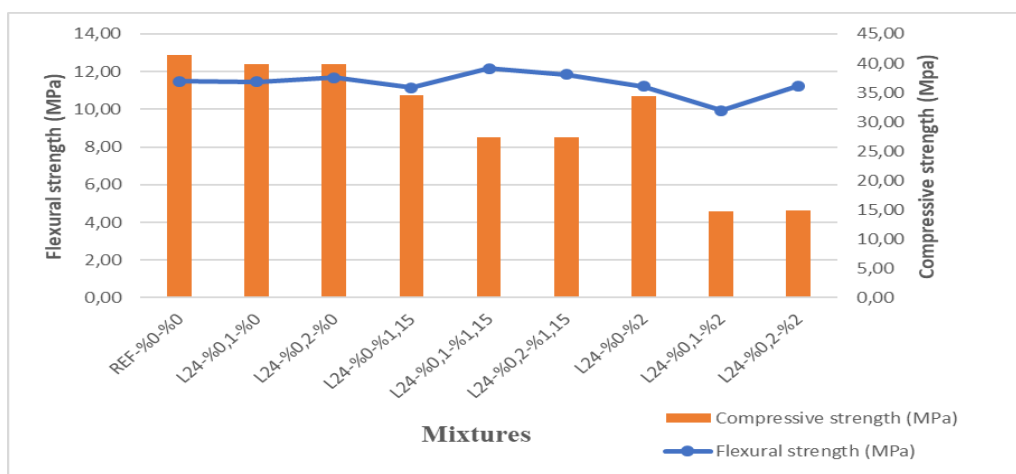


Figure 2. Compressive and flexural strength results

3.1.3. UPV

UPV values of mortar samples are shown in Figure 3. In the test, the transit time of ultrasonic sound through the specimen was measured. The samples with the dimensions of 4x4x16 cm were tested in terms of UPV. During the experiment, the transmission time was measured, and the length of the transmission path was divided by this value to calculate the ultrasonic pulse velocity. UPV values varied between 4.37-4.51 mm/μs. As the UPV fiber ratio increased, it was observed that the speed decreased, while the water impermeability added increased in speed.

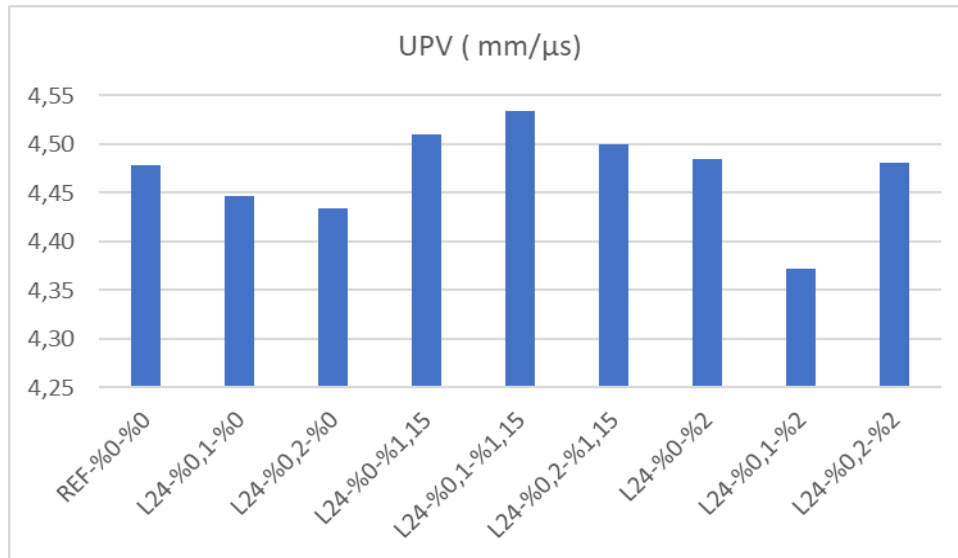


Figure 3. Results of UPV values of mortar samples

3.1.4. Splitting Tensile Strength

Splitting tensile strength values of mortar samples are shown in Figure 4. Splitting tensile test has been carried out in accordance with “TS EN 12390-6” [23]. Results in the tensile strength test in split increase compared to the reference samples. As the fiber ratio increased, the split tensile strength increased by 20% compared to the reference sample. There was a 50% increase compared to the reference sample in the series using impermeability additives.

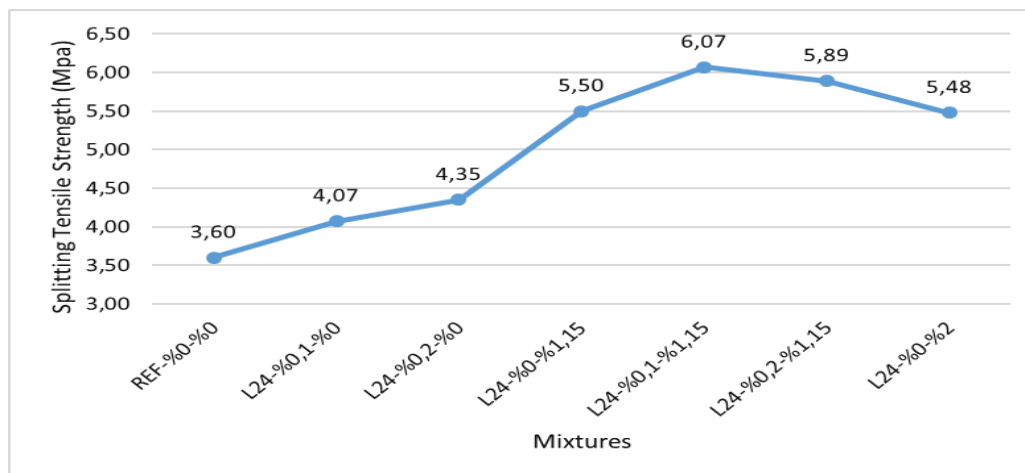


Figure 4. Results of splitting tensile strength values of mortar samples

3.1.5. Determination of water processing depth under pressure

The determination of water penetration depth under pressure was performed in accordance with the standard of TS EN 12390-8 [24]. Water treatment depth values of mortar samples are shown in Figure 5. While the water height in the reference sample was 12.33 mm, the lowest pressure water processing depth was measured as 10.67 mm in L24-0.2% -0% series. It is the series in which the water processing depth of 10.67 mm is the glass fiber ratio of 0.2%. This situation shows that the increase in fiber ratio leads to a decrease in water penetration depth. The depth of water under pressure was measured with the highest 13.38 mm in L24-0-2 series.

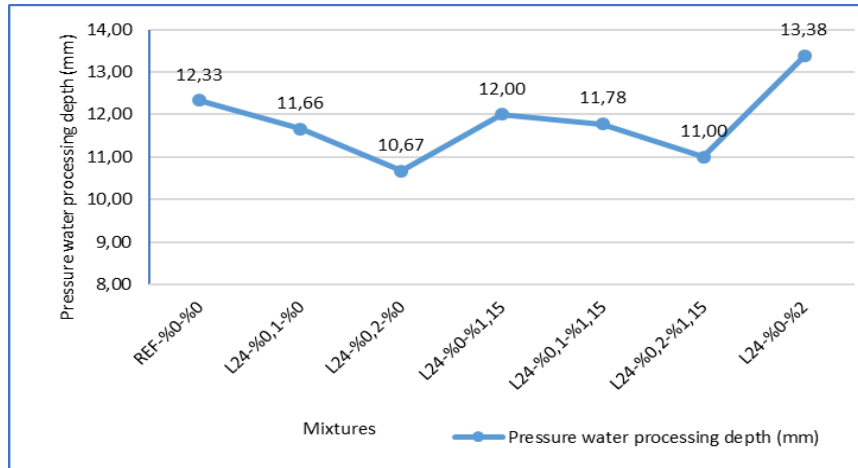


Figure 5. Results of water treatment depth values of mortar samples

4. Conclusions

In this study, the mechanical and permeability properties of glass fiber reinforced mortars were investigated. The study shows an improvement in mechanical properties for glass fiber reinforced mortar. The conclusions obtained from the experimental study are listed below:

1. When examined in terms of workability, the flow diameter decreased as the fiber ratio and impermeability contribution increased, the flow value decreased as the impermeability contribution increased.
2. A decrease in compressive strength was observed in series where fiber glass and impermeability additive were used together. The use of fiber glass and impermeability additive did not make any changes in terms of flexural strength.
3. In the series where the fiber glass is used at a rate of 0.1% by volume, the split tensile strength increased by 13% compared to the reference, while the split tensile strength increased by 20% compared to the reference when it was used at a rate of 0.2%. Glass fiber can be used in certain proportions in mortars where high tensile strength is required.
4. The depth of pressurized water penetration in L24-0.2% -0% series where the fiber glass ratio is 0.2% has reduced by 14%. The use of glass fiber positively affected the water penetration depth. In the mortar series where fiber glass and impermeability additive are used together, no significant change has been achieved in terms of pressurized water permeability.
5. As expected from fiber reinforced mortars the sudden collapse does not occur after crack formation.

Conflict of interest

The author declared no potential conflicts of interest with respect to the research, authorship, and/or publication of this article.

Data Availability Statement

All graphs and data obtained or generated during the investigation appear in the published article.

Ethics

There are no ethical issues after the publication of this manuscript.

References

- [1] Newman, J., & Choo, B. S. (Eds.). (2003). *Advanced concrete technology 3: processes*. Elsevier.
- [2] Kabay, N. (2014). Abrasion resistance and fracture energy of concretes with basalt fiber. *Construction and Building Materials*, 50, 95–101. <https://doi.org/10.1016/j.conbuildmat.2013.09.040>
- [3] B. Baradan , H. Yazıcı, S. Aydın. (2012). *Beton*, DEÜ Mühendislik Yayınları, İzmir.
- [4] Nataraja, M., Dhang, N., & Gupta, A. (2000). Toughness characterization of steel fiber-reinforced concrete by JSCE approach. *Cement and Concrete Research*, 30(4), 593–597. [https://doi.org/10.1016/s0008-8846\(00\)00212-x](https://doi.org/10.1016/s0008-8846(00)00212-x)

- [5] Yıldız, T., Yıldız, S., & Keleştemur, O. (2011). Cam Lif Katkılı Betonda Filler Malzemesi Olarak Atık Mermer Tozunun Kullanılabilirliğinin Araştırılması. *e-Journal of New World Sciences Academy*, 6(4),1A0239.
- [6] B. Bahadır. (2007), Concrete Fracture Toughness Impact of Life, SAE Institute of Science and Technology, Construction Education Department, Istanbul, Turkey [MSc Dissertation Thesis].
- [7] Demirel, B., & Yazıcıoğlu, S. (2010, May). ‘İnce Malzeme Olarak Kullanılan Atık Mermer Tozunun Betonun Mekanik Özellikleri Üzerine Etkisi. In *International Sustainable Buildings Symposium, Bildiriler Kitabı* (pp. 173-176).
- [8] Yehia, S., Douba, A., Abdullahi, O., & Farrag, S. (2016). Mechanical and durability evaluation of fiber-reinforced self-compacting concrete. *Construction and Building Materials*, 121, 120–133. <https://doi.org/10.1016/j.conbuildmat.2016.05.127>
- [9] Supit, S. W. M., & Shaikh, F. U. A. (2014). Durability properties of high volume fly ash concrete containing nano-silica. *Materials and Structures*, 48(8), 2431–2445. <https://doi.org/10.1617/s11527-014-0329-0>
- [10] Shaikh, F. U., & Supit, S. W. (2015). Compressive strength and durability properties of high volume fly ash (HVFA) concretes containing ultrafine fly ash (UFFA). *Construction and Building Materials*, 82, 192–205. <https://doi.org/10.1016/j.conbuildmat.2015.02.068>
- [11] Anandaraj, S., Rooby, J., Awoyera, P. O., & Gobinath, R. (2019). Structural distress in glass fibre-reinforced concrete under loading and exposure to aggressive environments. *Construction and building materials*, 197, 862-870. <https://doi.org/10.1016/j.conbuildmat.2018.06.090>
- [12] Hemavathi, S., Sumil Kumaran, A., & Sindhu, R. (2020). An experimental investigation on properties of concrete by using silica fume and glass fibre as admixture. *Materials Today: Proceedings*, 21, 456–459. <https://doi.org/10.1016/j.matpr.2019.06.558>
- [13] Jonalagadda, K. B., Kumar Jagarapu, D. C., & Eluru, A. (2020). Experimental analysis on supplementary cementitious materials with Alkali Resistant glass fibers. *Materials Today: Proceedings*, 27, 1569–1574. <https://doi.org/10.1016/j.matpr.2020.03.209>
- [14] Sanjeev, J., & Sai Nitesh, K. (2020). Study on the effect of steel and glass fibers on fresh and hardened properties of vibrated concrete and self-compacting concrete. *Materials Today: Proceedings*, 27, 1559–1568. <https://doi.org/10.1016/j.matpr.2020.03.208>
- [15] Afroughsabet, V., & Ozbakkaloglu, T. (2015). Mechanical and durability properties of high-strength concrete containing steel and polypropylene fibers. *Construction and Building Materials*, 94, 73–82. <https://doi.org/10.1016/j.conbuildmat.2015.06.051>
- [16] Neville, A.M. (1996). *Properties of Concrete*, 4th Ed., Wiley & Sons, New York.
- [17] TS EN 196 -1. (2016). *Methods of testing cement - Part 1: Determination of strength*. Turkish Standard Institute, Ankara, Turkey.
- [18] O. Karahan, C.D. Atis. The durability properties of polypropylene fiber reinforced fly ash concrete. *Mater. & Design*, 32: 1044-1049, 2011. <https://doi.org/10.1016/j.matdes.2010.07.011>
- [19] Shekarchi, M., Libre, N. A., Mehdipour, I., Sangtarashha, A., & Shafieefar, A. (2008). Shrinkage of highly flowable mortar reinforced with polypropylene fibre. In *The 3rd International Conference-ACF/VCA* (pp. 210-216).
- [20] Sun, Z., & Xu, Q. (2009). Microscopic, physical and mechanical analysis of polypropylene fiber reinforced concrete. *Materials Science and Engineering: A*, 527(1–2), 198–204. <https://doi.org/10.1016/j.msea.2009.07.056>
- [21] Puertas, F., Amat, T., Fernández-Jiménez, A., & Vázquez, T. (2003). Mechanical and durable behaviour of alkaline cement mortars reinforced with polypropylene fibres. *Cement and Concrete Research*, 33(12), 2031–2036. [https://doi.org/10.1016/s0008-8846\(03\)00222-9](https://doi.org/10.1016/s0008-8846(03)00222-9)
- [22] Venkata Krishna Bhargava, V., Brahma Chari, K., & Ranga Rao, V. (2020). Experimental investigation of M40 grade concrete with supplementary cementitious materials and glass fiber. *Materials Today: Proceedings*, 33, 519–523. <https://doi.org/10.1016/j.matpr.2020.05.209>
- [23] TS EN 12390-6. (2010). *Testing hardened concrete-Part 6: Tensile splitting strength of test specimens*, Turkish Standard Institute, Ankara, Turkey.
- [24] TS EN 12390-8. (2010). *Testing hardened concrete-Part 8: Depth of penetration of water under pressure*, Turkish Standard Institute, Ankara, Turkey.



Review Article

Pollution Free and Sustainable Copper Production Using Greenhouse CO₂

Subir Paul^{a,*}, Ramesh Chandra Das^a, Tamal Das^a

^aDepartment of Metallurgical and Material Engineering, Jadavpur University, Kolkata, India

Abstract

The objectives of the present investigation to decrease the global pollution by utilizing the CO₂ gas, in an effective way to produce the valuable metal copper, using low grade Cu ore which is termed as waste and not used for conventional Cu production. So the idea being waste and polluting waste are converted to useful products which will create employment, boost economy and reduce environment pollution. It is an innovative scheme for start-up. Carbonic acid produced by dissolving greenhouse gas CO₂ was used for leaching low grade chalcopyrite ore under oxidizing condition. It is a single stage process with a single reactor where combined hydrometallurgical and electrometallurgical process occur. At anode an oxidizing condition is produced by dragging electron thereby increasing the rate of hydrometallurgical extraction producing Cu⁺⁺ from CuFeS₂. This generated Cu⁺⁺ is simultaneously deposited at the cathode in the same reactor. The Cu produced was analysed and identified by RDR. The electrical power and energy consumption were computed. In the conventional Cu extraction process from CuFeS₂, sulphur come out as SO₂, the harmful polluting gas, in contrast in this process, sulphur came out as elemental sulphur and can be sold as by-product.

Keywords: Greenhouse Gas; Global Pollution; Sustainable Development; Cu Production; Hydrometallurgy

1. Introduction

Global environment pollution is due to the emission waste gases of burnt fuels from automobiles and manufacturing industries. Of these gases, Carbon dioxide is the main pollutant and is cause of global warming. In the developed countries, many industries had to be stopped due to government stringent laws against emission of the polluting CO₂. All nations in the developed and developing countries are involved and global pollution affected by one nation may be cause of gas emission of another nation. For over a century and half, such activities have pumped huge CO₂ into the atmosphere to increase its level higher than what have been for thousands of years. Though, governments of some pollution worried countries are taking measures to limit emissions of carbon dioxide and other greenhouse gases, the other countries are still emitting the harmful gases. It needs meeting of different nations and forming common laws to combat the problem. Thus, a voluntary agreement among 118 nations was made on November 4, 2016 [1], known as the Paris Agreement on environment pollution, to combat climate change. According to this agreement, each country agreed to take measures to combat climate change, with the ultimate goal of keeping the post-industrial global temperature rise below two degrees Celsius. Carbon tax [2] is another

This paper was recommended for publication in revised form by Editor Orhan Canpolat

* Corresponding author/E-mail address: spaul@metal.jdvu.ac.in (S. Paul)

<https://doi.org/10.29187/jsomt.2021.58>

Received 27 December 2018; Received in revised form 21 January 2020; Accepted 13 October 2020,

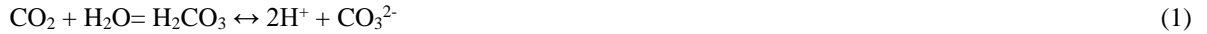
Available online 31 March 2021



method is cut down gas emission. In this case individuals and companies will have to pay higher taxes higher pollution generation process but will get incentives if they conserve energy and pollute less.

The present investigation aims at utilizing CO₂ and other harmful gases evolved in the atmosphere to produce useful products. That is waste to materials.

If CO₂ is passed through water carbonic acid is formed according to the following reaction.



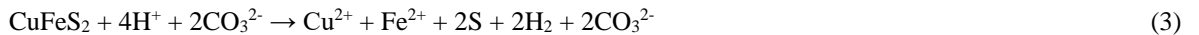
Carbonic acid is produced and further by hydrolysis, acid is generated and pH decreases of the system. How to utilize these two products?

Chalcopyrite ore, CuFeS₂, with Cu percentage less than 0.05% is not used for Cu production by conventional route. This low grade ore waste, obtained after mining and mineral beneficiation is dumped outside Cu extraction part and so only transportation cost is required to procure it.

Conventionally Cu is extracted from CuFeS₂ by pyrometallurgical route [3, 4], that is roasting and smelting, converting at high temperature, followed by Electrorefining. The first three processes generate another polluting gas SO₂ which is thrown into the atmosphere and is the main culprit for acid rain. Instead, if the chalcopyrite ore CuFeS₂ is hydrometallurgical extracted using by some solvent leachant [5], Sulphur will come as element sulphur S, which can be sold as by-product generation of SO₂ can be prevented. The reaction is as follows:



The reaction requires highly oxidizing condition to be maintained. Fe³⁺ is an oxidizing agent, but it reduces to Fe²⁺ after the reaction. To find the feasibility to utilize the green gas (1) for the above extraction of Cu (2), the reactions (1) and (2) need to be combined as follows:



Since Cu/Cu²⁺ system is more noble than H₂/H⁺ system, the reaction is feasible under oxidizing condition. Fe³⁺, an oxidizing agent, can be added to proceed the reaction to the forward direction, else the system can electrical oxidized by applying external potential to drag electron through electrode as discussed below.

1.2 Combining Hydro and Electro Metallurgical Process

In this concept [6], two conducting neural electrodes such as graphite are placed into the hydrometallurgical reactor. The one which acts as anode generates electron, producing oxidizing condition by the following reaction:



So the Fe²⁺ generated from the reaction (3) is oxidized back to Fe³⁺ by electrical oxidation ion the vicinity of anode.

At cathode Cu is deposited by the following reaction:



So the hydro and electro metallurgical processes occur simultaneously and in a single stage process Cu is produced. The applied potential and current from D C source works for oxidation at anode, favouring oxidizing condition in the vicinity of anode and reduction of Cu²⁺ to Cu at cathode for metal production. The potential should be controlled such that potential is sufficient to make reaction (5) occur but does not reduce H⁺ to H and Fe²⁺ to Fe.

The reversible electrode potential required for Cu deposition is given by Nernst equation as follows:

$$E_{re} = E_{0M} + 2.33RT/nF \log [M^{++}] \quad (6)$$

Where M stands for any metal Cu. E_0M is the standard electrode potential, E_{re} is the reversible potential Cu electrode potential, F = faraday, n = no of the electrons involved. At anode the following reaction occurs and the product of it produce oxidizing condition for the reaction (3) to proceed



The applied potential is for Cu deposition is much more than given by the equation (6), since over voltages need to be added as given by the following equation:

$$E = E_{eq} + \eta_{act} + \eta_{con} + IR_{elyt} \quad (8)$$

Where η_{act} = Overvoltage due to activation polarization or charge transfer electrode reaction, η_{con} overvoltage due to concentration polarization or mass transfer process by diffusion through the electrolyte, R_{elyt} resistance of the electrolyte.

Generally, for electrodeposition, the conductivity of the bath is made very high and the 3rd term of the equation may be neglected.

2. Experimental Methods

Low grade Chalcopyrite ore (0.05% Cu) was obtained (Figure 1) from Hindustan Copper Limited, Ghatshila, Jharkhand India. It was crushed and ground to -200 mesh. 20 gm of this ground ore was taken for each experiment. Polluting greenhouse gas CO_2 was generated by dropping dilute HCl over CaCO_3 as shown in Figure 2, experimental set up. Polluting gas was also produced by burning wood floor with air in an enclosed chamber as shown in the bottom part of Figure 2. The real pollution environment was used in the next stage of experiments after 1st set of experiment using pure CO_2 was successful in producing Cu.

The polluting gas was passed through the solution (200ml distilled water), containing ground sample of 2gm Chalcopyrite ore. Two graphite electrodes were pushed through the top of the reactor and D C potential was applied across. The current and potential applied were recorded by digital meters. The electrode, connected with +ve terminal acted as anode and it helps in oxidizing leaching of the reaction 3. The other electrode, connected with the -ve terminal acted as cathode where Cu was supposed to deposit from Cu^{2+} ions. Initially oxidizer Fe^{3+} ions were added to the solution to start the reaction.

3. Results and Discussion

The noble idea behind the present work is utilization of exhaust polluting gasses (mainly CO_2) from the plant (Figure 1) and low grade unused chalcopyrite ore. Both are wastes which are converted to valuables. So the aim is waste to economy. Figure 2 shows the details of experimental set up which was discussed in the previous section.

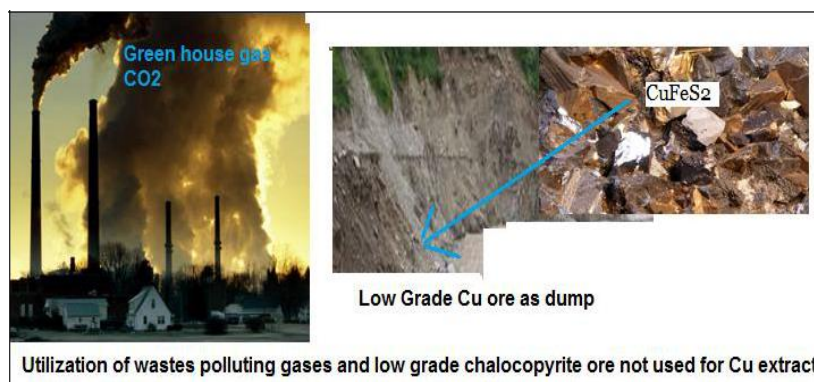


Figure 1. Emission of polluting CO_2 gas used to produce Cu collected from waste

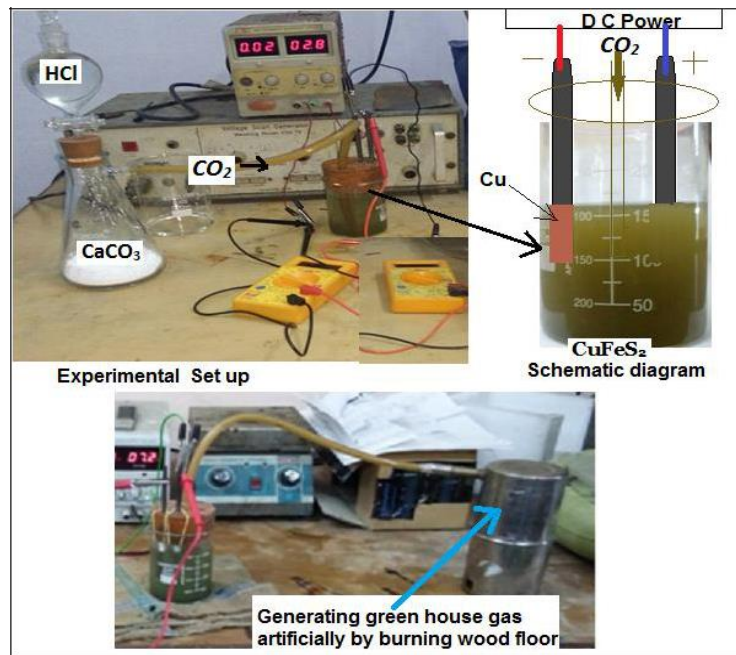


Figure 2. Experimental set up to extract Cu, using CO₂ generated from carbonate or Burning wood floor, by combined Hydro and Electro Metallurgical Process

It was found that after the experiment, the color of the solution turns yellow (Figure 3). This is due to release of elemental sulphur S as explained by the reactions (2) and (3) above. The solution was filtered and the residue (Sulphur) was dried to obtain sulphur as by-product. In the conventional process of Cu extraction from CuFeS₂, sulphur comes out as SO₂ gas which is thrown into the atmosphere, aggravating environment pollution. In the present process, not only this pollution problem is prevented, but sulphur comes out as product to sell and increase economy.

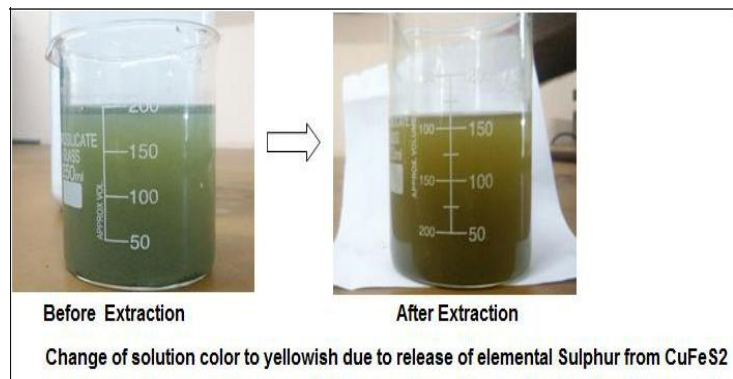


Figure 3. Showing yellowish solution due to release of elemental Sulphur

Figure 4 shows the Cu extracted at different temperature, both by hydrometallurgy and electrometallurgy. Cu²⁺ ions, first comes out from CuFeS₂ into the solution by reacting with carbonic acid, produced from CO₂ gas (reaction 3). This is hydrometallurgical extraction of Cu. It requires an oxidizing condition. Initially it is provided by adding Fe³⁺ ions. But once the reaction starts, the anodic region gets oxidized as electrons are dragged through anode, with the reaction (4), when Fe³⁺ ions are regenerated, maintaining oxidizing condition at cathode the release Cu²⁺ ions are converted to metallic Cu. Thus, when Cu extracted by hydrometallurgy falls, Cu extracted by electrometallurgy rises.

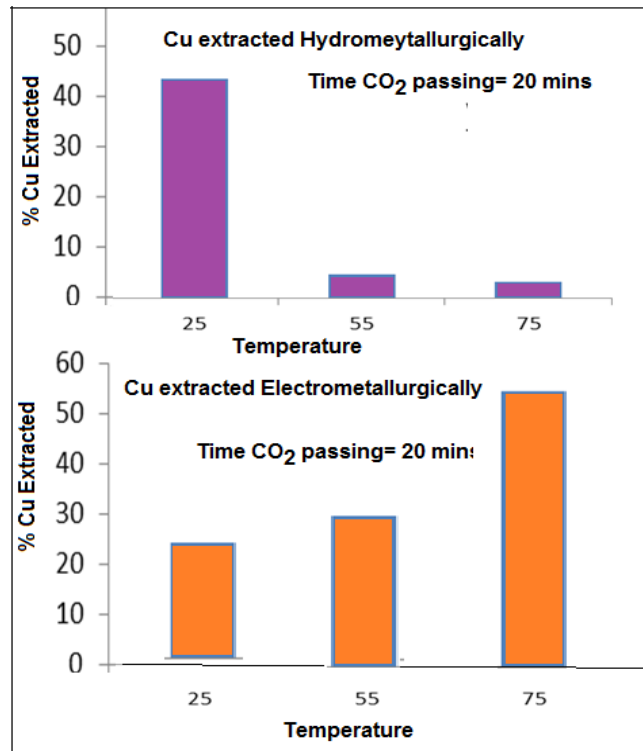


Figure 4. Bar graph showing metal extracted by Hydrometallurgy and Electro metallurgy with variation of temperature of leaching by CO₂

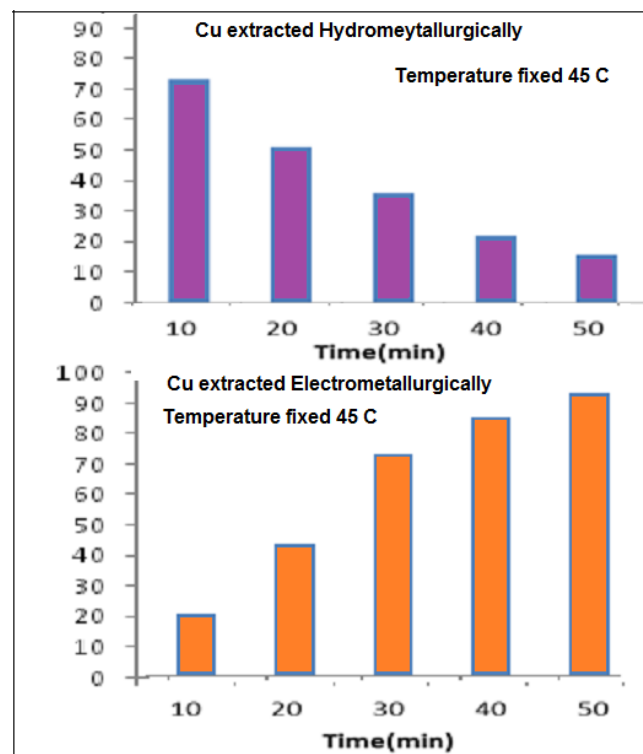


Figure 5. Bar graph showing metal extracted by Hydrometallurgy and Electrometallurgy with variation of the time of extraction by CO₂

Figure 5 shows similar study as the function of time of CO₂ gas passing, at fixed temperature of experiments. The bar shows at each time (say 30 min.), the addition of two bars values will give the total amount of Cu extracted during that time by the combined hydro and electrometallurgical process.

This is illustrated in Figure 6 which shows combined hydro and electro metallurgical extraction of Cu (green line curve) with passage of CO₂ passing. It is seen that with passage of time the Cu amount by hydrometallurgy decreases, while that by

electrometallurgy increases. So the Cu^{2+} released by hydrometallurgy is immediately deposited at graphite cathode. The XRD of the deposited Cu at cathode is shown in Figure 7, which exhibits the presence of Cu, along with some CuO .

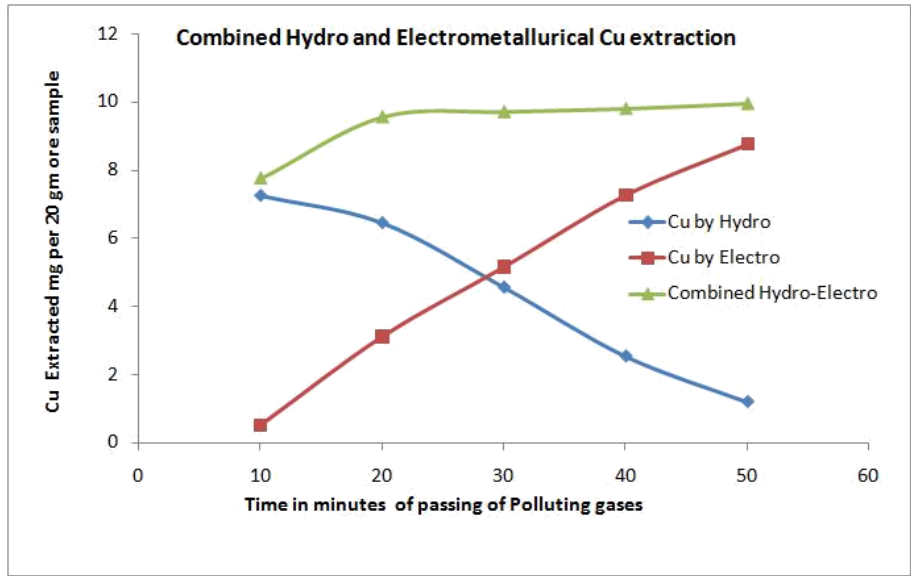


Figure 6. Comparison of Cu Extracted by Hydrometallurgy, Electrometallurgy and combined

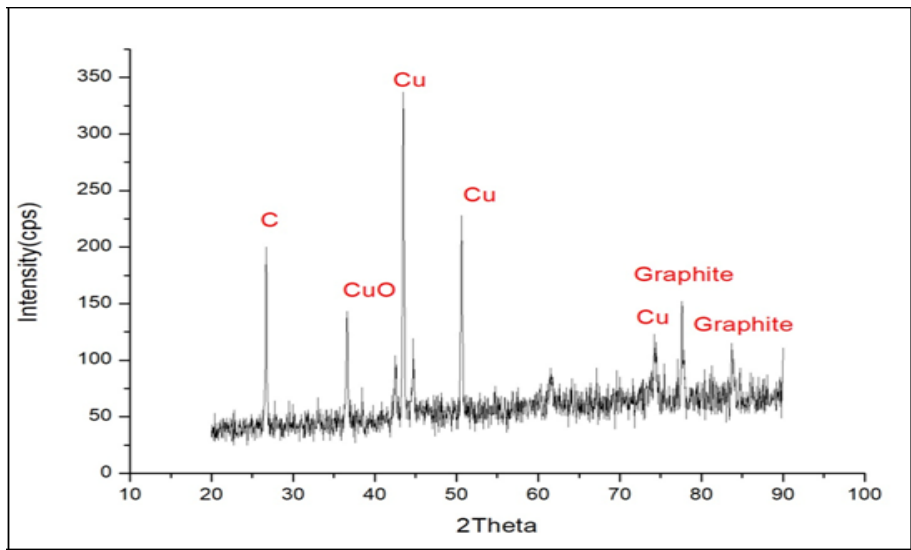


Figure 7. XRD of Electrodeposited Cu

The applied potential between the two electrodes was 2.0-3.0 volt, depending on the temperature of operation and the applied current density was 3- 5 mA/cm^2 . Figure 8 shows the power consumption and energy required for Cu production by combined hydro and electro metallurgical process using the greenhouse gas.

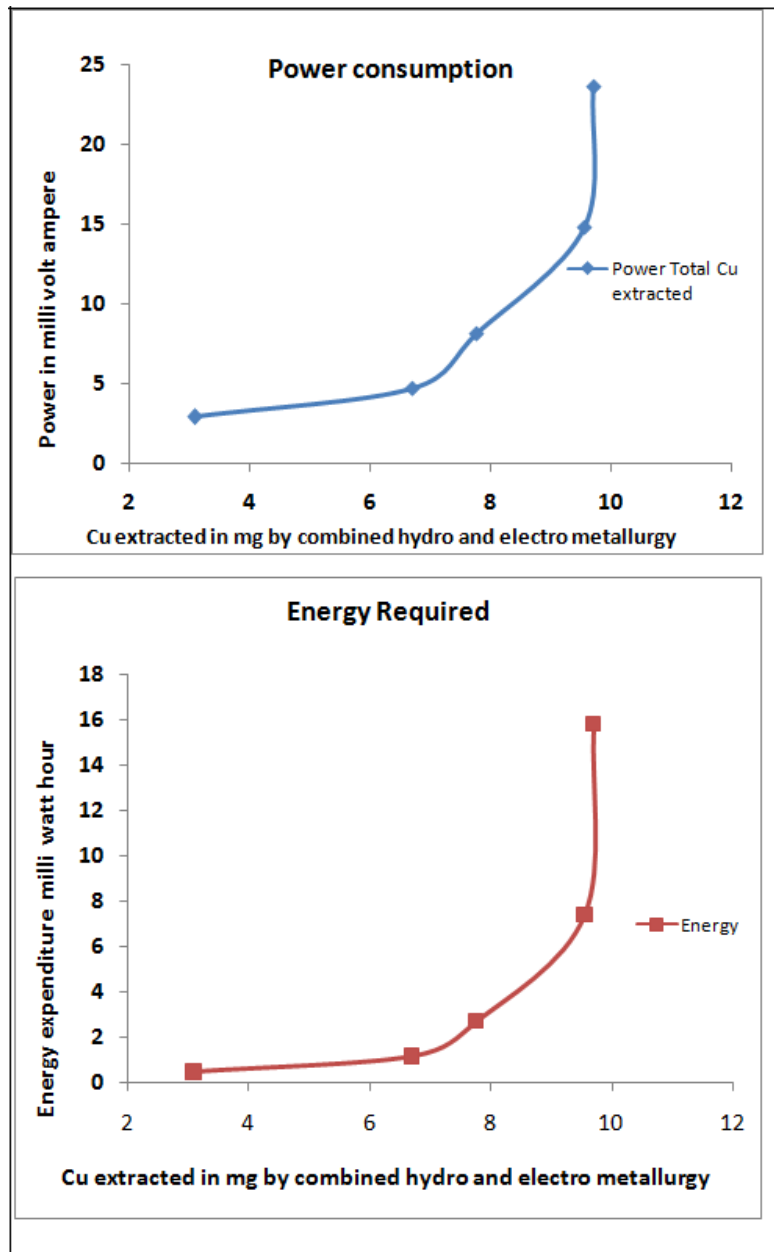


Figure 8. Power and energy consumption of amount of extracted Cu

4. Conclusion

Cu production could be achieved from low grade Cu ore, using environment polluting greenhouse gases with an energy intensive process of a single stage combined hydro and electro metallurgical process.

Conflict of interest

The authors declared no potential conflicts of interest with respect to the research, authorship, and/or publication of this article

Ethics

There are no ethical issues after the publication of this manuscript.

References

- [1] Egypt, M. (2001) Multipurpose Forest Management Plans Based on Geographic Information Systems Purpose Programming Method (Forestry Planning Planning Example), Ph.D. Thesis, KTU Graduate School of Natural and Applied Sciences, Trabzon.
- [2] Akay, A. E., Erdas, O., Belen, B. (2006). Using GIS-Based Sediment Estimation Model, SEDMODL2 in Calculation of Sediment from Forest Roads. Workshop made of forestation and erosion control applications in semi-arid regions of Turkey.
- [3] Altun, L., Yilmaz, M., Acar, C., Turna, I., Başkent, E. Z., & Bilgili, E. (2003). Evaluating the seasonal changes of water quality of the Değirmendere and Galyan Rivers (Trabzon, Turkey). *Journal of Environmental Biology*, 24(4), 415-422.
- [4] Başkent, E. Z. (2001). Combinatorial optimization in forest ecosystem management modeling. *Turkish Journal of Agriculture and Forestry*, 25(3), 187-194.
- [5] ETABS V13. Computers and structures Inc. New York, NY 10036, USA
- [6] ACI 209R-08. (2008). Guide for Modelling and Calculating Shrinkage and Creep in Hardened Concrete. American Concrete Institute, USA.